



Refined dataset to describe the complex urban environment of Hong Kong for urban climate modelling studies at the mesoscale

Yu Ting Kwok¹ · Cecile De Munck² · Robert Schoetter² · Chao Ren³ · Kevin Ka-Lun Lau⁴

Received: 29 September 2019 / Accepted: 8 June 2020
© Springer-Verlag GmbH Austria, part of Springer Nature 2020

Abstract

Urban climate models are indispensable tools for the evaluation of climatic risks faced by the growing urban population. In order to accurately simulate the urban surface energy balance at a high spatial resolution, it is important to provide models with detailed input data that can adequately describe the spatial variation of land covers, urban morphology, construction materials, and building functions within an urban area. Using Hong Kong—a city well-known for its complex, high-rise urban environment—as the testing ground, this study aims to present a geographic information system–based workflow for the construction of a refined urban database. Firstly, maps of land cover tiles, pervious and impervious surface fractions, building height, and other input parameters required by mesoscale atmospheric models are derived from multiple data sources including administrative building data, satellite images, and land use surveys. Secondly, a total of 18 representative building archetypes, with their corresponding architectural characteristics and occupant behaviour schedules, are defined. This allows for models to take into account the radiative, thermal, and dynamic interactions between buildings and the atmosphere, as well as the anthropogenic heat fluxes. Finally, locally adapted ranges of urban morphological parameters for the different local climate zones (LCZs) are derived, enabling the expansion of data coverage to neighbouring areas of Hong Kong, where detailed urban data are not readily available. Uncertainties of the refined database and limitations of the LCZ scheme are also discussed so that a similar approach may be adapted and applied to other cities in the world.

1 Introduction

In the past few decades, the urban climate modelling community has made tremendous progress in improving the representation of the surface energy balance (SEB) in urban areas (Garuma 2018). As a result, a profusion of atmospheric

models operating at different scales and coupled with urban land surface models (ULSMs) with different levels of complexity is available. Urban canopy models (UCMs), such as the Town Energy Balance (TEB; Masson 2000), the single-layer UCM developed by Kusaka et al. (2001), and the multi-layer building effect parameterisation (BEP; Martilli et al. 2002), are now commonly employed to simulate the urban SEB. They solve separately (and at different atmospheric levels for BEP) the energy budgets for walls, roofs, and roads, as opposed to earlier empirical models and modified vegetation schemes, which treated urban areas as flat slabs with large roughness length, uniform temperature, high thermal capacity, and low surface albedo (Masson 2006). Based on the results of 32 ULSMs in the international model comparison project, Best and Grimmond (2015) concluded that a minimum requirement for ULSMs is to simulate the changes in bulk surface albedo due to building material properties and urban canyon geometries, the differences in upward longwave radiation between street canyons and on top of roofs, and the evapotranspiration by urban vegetation. Besides, the inclusion of anthropogenic heat fluxes (QH) have been found to have significant impacts on urban SEB modelling (Fan and Sailor

Electronic supplementary material The online version of this article (<https://doi.org/10.1007/s00704-020-03298-x>) contains supplementary material, which is available to authorized users.

✉ Yu Ting Kwok
ytkwok@link.cuhk.edu.hk

- ¹ School of Architecture, The Chinese University of Hong Kong, Hong Kong, China
- ² CNRM, Université de Toulouse, Météo-France, CNRS, Toulouse Cedex 1, France
- ³ Faculty of Architecture, The University of Hong Kong, Hong Kong, China
- ⁴ Institute of Future Cities, The Chinese University of Hong Kong, Hong Kong, China

2005; Ohashi et al. 2007). This can be achieved by further coupling the ULSM with a building energy model (BEM; Kikegawa et al. 2003; Salamanca et al. 2010; Bueno et al. 2012) and parameterising human behaviour related to building energy consumption (Schoetter et al. 2017).

Apart from the selection of appropriate urban parameterisation schemes, the quality and precision of model input data describing the surface cover and three-dimensional (3D) characteristics of urban areas also contribute to the realism of model outputs (Holt and Pullen 2007; Grimmond et al. 2011; Salamanca et al. 2011; Monaghan et al. 2014; Wong et al. 2019). When USLMs move away from bulk representations of the urban surface, the spatial variability of the urban form and function within a city needs to be adequately described. However, the lack of such detailed geophysical and socioeconomic data is impeding the routine application of UCMs in urban climate modelling and thus the realistic assessment of the climatic hazards faced by the urban population, as stated in the last IPCC Assessment Report (Revi et al. 2014). Therefore, considerable efforts have been made to establish global and regional databases describing land covers, urban morphology, and building typologies. The advancement in remote sensing technologies has facilitated the production of a spectrum of land cover products with various classification schemes and spatial resolutions (review by Grekousis et al. 2015). Often, there is only one single class for built-up or artificial surfaces. To take into account the complexity of urban surfaces and the heterogeneity of built forms, recent initiatives have been launched to provide a refined description of urban areas. For example, Jackson et al. (2010) compiled a dataset at a 1-km resolution that captures global variations in urban intensity, building morphology, and their thermal and radiative properties, for its application in global climate modelling. Another example is the Global Human Settlement Layer framework which provides detailed information on the spatio-temporal evolution of worldwide settlements and urbanisation by a fully automatic workflow at up to a 38-m resolution (Pesaresi et al. 2016). The World Urban Database and Access Portal Tools (WUDAPT; Ching et al. 2018) is another ongoing initiative to develop a worldwide consistent database for urban climate studies. It employs the local climate zone (LCZ) scheme (Stewart and Oke 2012) for the consistent mapping of ten urban classes and seven land cover classes based on their physical properties and thermal climatic influences. Furthermore, the approach of using building typologies for obtaining architectural and energy-related building data has been adopted in 20 European countries (Loga et al. 2016). French building archetypes, defined by their type, function, age, and location (a.k.a. the GENIUS approach), have been employed in TEB-BEM to provide model input parameters for building facade characteristics and construction material properties (Tornay et al. 2017). Models to estimate global anthropogenic heat

emissions have also been developed, such as LUCY (Allen et al. 2011) and the AHE database by Dong et al. (2017), providing information on the QF, which is a component of the SEB specific to urban areas.

These global and regional datasets obtained from top-down methods are able to provide a first estimate of the parameters required by UCMs. However, as urban land use, morphology and building characteristics can vary significantly between cities with different physical geography and cultural backgrounds (Jackson et al. 2010; Sabo et al. 2018), generic look-up tables, such as that proposed by Stewart and Oke (2012) for LCZs, may not be equally suited for all cities. There is evidence demonstrating how poorly chosen parameter values could undermine the performance of models with good model physics (Grimmond et al. 2011). The urban environment can also vary significantly within a city and such details are often difficult to be captured by regional datasets. Hence, for local scale studies, the use of locally adapted and spatially detailed urban datasets is essential (Alexander et al. 2015; Jia et al. 2015; Hidalgo et al. 2019; Wong et al. 2019). These might be derived from real building information, an example being the lidar-based NUDAPT data (Ching et al. 2009).

Hong Kong is of great interest to the urban climate modelling community because of the multitude of challenges presented by both its natural and urban landscapes. Ranging from compact high-rise built-up areas to rural areas with steep hills and outlying islands within a mere 1100 km² of land, the surface cover is complex and heterogeneous. Hong Kong has a subtropical monsoonal climate and a strong maritime influence, resulting in hot and wet summers, and mild winters. The city ranks sixth worldwide in urban population density (Cox 2019) and intense human activities have led to a very high QF of up to 600 W/m² on average in commercial areas on an autumn day (Wong et al. 2015) and even higher values should be expected in summer. Previous modelling studies (at 4-km and 1-km spatial resolutions) have shown the effects of rapid urbanisation in Hong Kong and its neighbouring cities on temperature, wind, and precipitation in the Pearl River Delta (PRD) region (Wang et al. 2014; Tse et al. 2018). Using the Weather Research and Forecasting (WRF) model, they have found an increase in air temperature (1–2 °C) and a reduction in urban wind speed (up to 2 ms⁻¹) relative to the 1990s. At a finer spatial resolution of 500 m, Wang et al. (2017, 2018b) have employed the multi-layer BEP to include the dynamic and thermal effects of high-rise buildings in urban climate simulations of Hong Kong during high pollution and heatwave scenarios. However, these studies generally lack a detailed description of the complex urban environment of Hong Kong—they adopt only a categorical approach (i.e. three urban categories in the United States Geological Survey land-cover classification) and

give no local specification on parameters related to building materials and occupant behaviour.

As cities strive to become more resilient and to mitigate the changing climate, urban climate studies are needed to inform urban planning and policymaking. Such applications require the quantification and understanding of local climate variations at fine spatial scales down to the neighbourhood level. With the goal to provide a refined and complete urban database for mesoscale (100 m to few kilometers) urban climate simulations of the high-density, high-rise city of Hong Kong, the following objectives will be addressed in this paper:

1. To recall the input parameters that are required for urban climate modelling at the mesoscale (Section 2);
2. To present the workflow for the preparation of detailed input data describing the surface covers and urban geometry of Hong Kong (Section 3);
3. To define building archetypes and their respective model inputs related to building architecture and occupant behaviour for Hong Kong and discuss the global applicability of the approach (Section 4); and
4. To develop locally adapted ranges of urban morphological parameters for the different LCZs and discuss the relevance of the LCZ scheme for characterising the urban environment of Hong Kong (Section 5).

2 Overview of urban parameters for mesoscale atmospheric models

The spatio-temporal evolution of the urban form and function of cities needs to be captured for understanding the urban SEB through urban climate modelling. With reference to Masson et al. (2020), the surface input parameters relevant for describing cities in mesoscale atmospheric models and UCMs can be grouped into parameters describing land covers, urban surfaces and morphology, building construction materials, and occupant behaviour, ordered in increasing level of detail. Though the specific input data requirements may differ from one model/study to another, depending on model refinement and study objective, this section presents an overview of the common surface input parameters expected for urban climate modelling studies at the mesoscale.

2.1 The tile approach for land cover parameters

The energy, water, and momentum exchanges between the land surface and the atmosphere are strongly influenced by surface covers with different biophysical properties. For example, evapotranspiration is active on vegetated surfaces, resulting in higher latent heat fluxes, while heat storage and sensible heat fluxes are enhanced in built-up areas with

construction materials and impervious surfaces. Zhao and Wu (2018) showed a consistent increase in Bowen ratio (sensible heat flux to latent heat flux) over areas that experienced a land cover change from non-urban to urban in three city clusters in China. Another study found that in the tropical city of Putrajaya, Malaysia, replacing water and vegetated surfaces by urban surfaces could induce an increase in air temperature, and thus urban heat island (UHI) intensity, of 0.14 °C and 0.39 °C, respectively (Morris et al. 2016). Hence, it is important to account for the effects of land surface heterogeneity in atmospheric models. Evidence has shown that even for urban climate simulations conducted at fine grid resolutions (at or below 1 km), sub-grid land cover heterogeneities remain important and should not be neglected (Li et al. 2013). To this end, a tiling/mosaic approach that describes each model grid by a finite number of sub-grid tiles with homogeneous surface characteristics has been proposed (Avisar and Pielke 1989). Assuming all tiles receive the same atmospheric forcing, the SEB is calculated separately within each tile using respective land surface schemes and the resultant fluxes are aggregated before feeding back to the atmospheric model. This approach has been implemented in the Weather Research and Forecasting (WRF)-Noah modelling system and has been found to better capture the surface energy balance, especially the latent heat flux in urban areas (Li et al. 2013). Apart from the contrasts in surface characteristics for urban and vegetated areas, different types of hydrological features should be considered. Examples of other models adopting the tiling approach include the Externalised Surface scheme (SURFEX) with four surface tiles, namely Town, Nature, Sea, and Water (Masson et al. 2013), and the Community Atmosphere Model (CAM)-Community Land Model (CLM) with five land units, namely Glacier, Lake, Wetland, Urban, and Vegetated (Oleson et al. 2010). With a detailed land cover database like ECOCLIMAP (Masson et al. 2003), the surface cover fractions for the required tiles can be readily obtained at the global scale.

2.2 Specificities of urban surfaces and morphology

Within a tile of urban land cover, an USLM dedicated to resolving the interactions between the urban fabric and the atmosphere is employed. Owing to the three-dimensionality of urban surfaces and the properties of construction materials used, the natural SEB is strongly modified to create a so-called 'urban climate', manifested in phenomena such as the well-documented UHI (Oke 1981). On the one hand, both incoming shortwave radiation and terrestrial longwave radiation are retained within street canyons due to multiple reflections and reduced sky view factor. On the other hand, the amount of heat stored within street canyons is increased because of the high heat admittance of building construction materials. The configuration of urban settings also modifies the air flow and

trap pollutants within street canyons. Moreover, human activities in urban areas release heat and moisture to the atmosphere. It is therefore essential to define appropriate parameters describing the urban surfaces and morphology, as well as the materials which they are made of and the QF which they generate.

Spatial heterogeneity in surface covers continues to exist at smaller scales within urban environments. To simplify the urban morphology, most UCMs adopt an urban canyon approach, i.e. a road bordered by two facing building walls, as proposed by early urban climatologists (e.g. Oke 1987). Clearly, buildings form an important component of UCMs. Thus, the surface fraction of buildings within a model grid is a key input parameter needed for all UCMs. Within the street canyon, the surface cover may be impervious (i.e. roads and pavements) and/or pervious (i.e. vegetation and soil). Impervious and pervious surfaces possess distinctly different thermal and radiative properties and therefore should be separately defined in UCMs. Urban vegetation influences the energy fluxes within an urban street canyon through various physical processes including but not limited to, cooling by evapotranspiration, shading, and ventilation (Shashua-Bar and Hoffman 2000; Santamouris et al. 2018). Recent improvements of UCMs allow for the representation of different types of urban vegetation (e.g. urban parks, lawns, street trees, green walls/roofs) to achieve a more realistic simulation of the urban microclimate (Lemonsu et al. 2012; de Munck et al. 2013; Vahmani and Ban-Weiss 2016; Redon et al. 2017). Note that for mesoscale atmospheric models using the tiling approach, the surface fractions for building, impervious, and pervious covers may be defined as a function of the urban tile only, instead of the entire model grid, depending on the specific model input requirements.

The 3D geometry of urban areas often has a more significant impact on the urban thermal climate compared to 2D urban surface covers (Tian et al. 2019). Since a lot of the heat, momentum, and moisture exchanges between the city and the atmosphere take place at the wall-atmosphere interfaces, the wall density, defined as the ratio of the total vertical surface area of walls to the horizontal grid surface area, is a highly relevant input parameter for UCMs (Masson et al. 2020). Building height is strongly linked to the wall surface density as well as the volume of air obstructed by buildings. It is therefore a key input parameter for UCMs. The canyon aspect ratio and road width are two other commonly required input parameters to specify the street canyon geometry (Kusaka et al. 2001). However, when adopting a simplified urban canyon approach, these morphological parameters may not need to be independently defined, but can be deduced from others (Masson et al. 2020). In relation to the dynamic effects of built structures, the aerodynamic roughness length is required by UCMs. It describes the friction the urban surfaces exert on the atmospheric air flow. It can be measured in the field but

methods have been developed to estimate the roughness length in cities based on empirical relationships with the properties of surface roughness elements (Grimmond and Oke 1999). For a multi-layer model such as the BEP (Martilli et al. 2002), the vertical distribution of built density and the frontal area density (which depends on the direction of air flow) are required in place of inputs on the building height and roughness length. Indeed, the modification of the wind velocity and turbulent kinetic energy due to the building drag is parameterised as a function of these parameters (Dupont et al. 2004). With this approach, only a small value for the roughness length is used which represents the obstacles at the surface not accounted for by the drag force approach. The input parameters described here require higher spatial details compared to the land surface cover tiles. Common methods to obtain or derive these parameters include remote sensing (e.g. Bonczak and Kontokosta 2019), crowdsourcing (e.g. Ching et al. 2019), geographic information system (GIS) processing of administrative databases (e.g. Ching et al. 2009; Bocher et al. 2018), and deep learning techniques (e.g. Gong et al. 2018). Input parameters may be precisely defined for grids of a chosen resolution, or representative values may be set for a finite number of typical urban categories. The former requires a set of model input maps to specify all the urban parameters, while the latter requires only one input map of the distribution of urban categories, as in the WRF urban modelling system (Chen et al. 2011).

2.3 Representation of building characteristics

Building architectural characteristics impact the radiative and conductive heat transfer between buildings and the atmosphere. In particular, the albedos and insulation configurations for walls and roofs are highly influential to the urban SEB (Tornay et al. 2017). Other relevant parameters include the thermal conductivity, the heat capacity, and the thickness of the different construction materials for walls and roofs, including those of external/internal coatings. Simple BEMs are often further coupled to UCMs to model the energy budget of a representative building and to estimate the energy consumption at neighbourhood scale (Kikegawa et al. 2003; Salamanca et al. 2010; Pigeon et al. 2014). The BEM solves the energy budget of the indoor air taking into account the influence of intermediate floors, internal heat loads, (mechanical) ventilation, and windows, such that the QF due to building heating/cooling may be simulated. Windows not only possess radiative and thermal properties different to walls, but also have direct impacts on the air exchange through ventilation. Therefore, window types and glazing ratios need to be properly defined. Many city-scale mitigation/adaptation strategies for climate change could also be implemented by changing building architectural characteristics (e.g. painting roofs white; Santamouris 2014) and occupant behaviour (e.g.

increasing the cooling setpoint temperature; Li et al. 2012). Having information on buildings is therefore essential for fine-scale urban climate simulations.

Since it is not practical to define unique architectural characteristics for each building within a model grid, these parameters may be predefined based on representative buildings in a study region (building archetypes). For example, Tornay et al. (2017) defined for France these parameters as a function of the building type, building function, building age, and different geographic regions. Building energy-related parameters, including the cooling/heating setpoint temperatures, building occupancy schedules, and internal heat release, may be inferred directly from the building function. Recent model advancements in TEB have also made it possible to take into account the mix of multiple uses within a single building type (Schoetter et al. 2017). An alternative simpler approach to consider the building material and energy-related parameters in urban climate simulations is to set representative values for the same urban categories used for urban morphology and assign them to respective model grids based on a look-up table (Chen et al. 2011). However, this approach might introduce large uncertainties, since the link between urban morphology and construction material or energy-related parameters might not be robust.

A non-exhaustive list of typical urban surface input parameters applicable to different modelling approaches is presented in Table 1, and the hierarchy of the various parameters is displayed in Fig. 1, taking as an example the coupling between the non-hydrostatic mesoscale atmospheric model MesoNH (Lac et al. 2018), the surface model SURFEX (Masson et al. 2013) including the Town Energy Balance (TEB; Masson 2000), and the Building Energy Model (BEM; Bueno et al. 2012).

3 Construction of a refined urban database for Hong Kong

3.1 Detailed surface cover of Hong Kong

First, a detailed surface cover map is constructed for Hong Kong at the finest spatial resolution achievable, both in terms of raw data resolution and reasonable computing time. Data collected from various sources are processed and compiled on the GIS platform ArcMap 10.6.1. The coastline of Hong Kong is taken as to be the same as the administrative boundary of the Hong Kong Special Administrative Region, except for the northernmost boundary which is shared by Shenzhen of Mainland China. Shapefiles representing the current situation of buildings, roads, inland water features (e.g. rivers, ponds, swimming pools, reservoirs), land surface features (e.g. beaches, boulder outcrops), and other points of interest (e.g. cultivated land, burial grounds, recreational facilities) are

obtained from the Hong Kong Lands Department. Building polygons were last updated in May 2019, whereas other layers are as of 2016.

Information on vegetation is retrieved from two cloudless bottom-of-atmosphere reflectance images taken on 25 January 2019 by the Sentinel-2A satellite at a spatial resolution of 10 m (ESA 2019). Since the majority of vegetation in subtropical Hong Kong belongs to evergreen species, seasonal variation in vegetation coverage is assumed to be insignificant. The presence and density of vegetation is determined from the normalised difference vegetation index (NDVI), where pixels with an NDVI between 0.2 and 0.8 are classified as low/sparse vegetation (e.g. grassland, shrubland, farmland) and pixels with an NDVI over 0.8 and approaching 1 are classified as high/dense vegetation (e.g. woodland). These thresholds are adjusted and set such that the proportion and distribution of low and high vegetation can best reflect the real situation shown on the land utilisation map produced by the government (HKPlanD 2016) and with reference to a previously conducted urban tree survey. Although there exist more advanced image treatment techniques and vegetation type and fraction retrieval methods from satellite imagery (e.g. Jiang et al. 2006; Krüger et al. 2018), the simple approach taken here is considered sufficient to capture the urban vegetation characteristics in Hong Kong. Another advantage is that it can be easily transposed to other territories in the absence of data, which is often the case with vegetation.

All data layers are rasterised and resampled to a uniform spatial resolution of 1 m. The raster datasets are ‘mosaicked’ together in the GIS with priorities given to layers with a higher level of certainty: building > sea > road > inland water > vegetation > other urban (impervious covers including airport runways, cemeteries, container ports, piers, carparks). Remaining unclassified pixels (< 2% of all pixels) are treated as pavements and bare soil for urban and rural areas, respectively. Finally, areas associated with a vacant land use, mainly at sites undergoing (re)development (e.g. the Hong Kong Port of the Hong Kong-Zhuhai-Macao Bridge, the former Kai Tak Airport), are manually corrected with the help of georeferenced Google Earth satellite images. Based on the resultant 1-m raster of surface covers in Hong Kong (Fig. 2), the input parameters for describing land cover and urban surfaces in mesoscale models and UCMs (Table 1) can then be calculated at the required grid resolutions.

3.2 Land cover tiles within a model grid

In this paper, the maps of common input parameters required for mesoscale urban climate modelling studies are presented with a spatial resolution of 100 m. This grid size may be adjusted according to the precision of raw datasets as well as the scale and purpose of the study. The maps are constructed for the region of interest (ROI) encompassing Hong Kong

Table 1 Typical urban surface input parameters expected for urban climate modelling studies employing mesoscale atmospheric models coupled with UCMs

Input parameter	Description	Applicable for
Land covers		
Nature tile	Fraction of natural/rural areas; modelled using a soil-vegetation-atmosphere transfer (SVAT) scheme	Tiling/mosaic approach
Urban tile	Fraction of urban areas; modelled using an ULSM	
Sea tile	Fraction of sea/ocean	
Inland water tile	Fraction of inland hydrological features, e.g. lakes, rivers, wetlands	
Glacier tile	Fraction of glaciers/snow-capped surfaces	
Urban surfaces and morphology		
Building fraction	Fraction of buildings, i.e. the building plan area density	Single-layer UCMs
Impervious surface fraction	Fraction of impervious surfaces (e.g. roads, paved grounds) in the urban environment	
Pervious surface fraction	Fraction of pervious surfaces (may be further separated into surfaces with urban vegetation and bare soil) in the urban environment. There may also be a 'high vegetation' fraction defined to represent tree canopies above the ground.	
Average building height	Average height of buildings within a model grid, weighted by building footprint; both arithmetic (for energetic aspects) and geometric (for a representative height of roughness elements) average heights may be calculated	
Roughness length	An aerodynamic parameter to describe the air flow above a surface; may be estimated from the average and variations of building heights	
Wall density	Ratio of the total vertical surface area of walls to the horizontal surface area	
Canyon aspect ratio	Ratio of building heights to canyon/road widths (H/W)	
Vertical distribution of built density	Fraction of buildings at different atmospheric model levels	Multi-layer UCMs (drag force approach)
Frontal area density	Vertical surface area of windward walls over an horizontal surface area for a certain wind direction	
Urban category	Typical urban setting with associated representative surface fraction and morphological input parameters for UCMs, e.g. low/high-intensity residential and industrial/commercial, or LCZs	Categorical approach for UCMs
Building characteristics		
Building type	Dominant building type (e.g. high-rise building, informal building) within a model grid; useful for inferring building architectural characteristics	Categorical approach for BEMs
Building function	Dominant building use (e.g. residential, commercial, medical, educational) within a model grid; useful for inferring building energy-related parameters	
Building age	Dominant construction period of buildings within a model grid; useful for inferring building thermal regulations	
Geographic region	Information on where the buildings are located in; useful for inferring building construction material	

Island, Kowloon Peninsula, and three of the most populated new towns Tsuen Wan, Sha Tin, and Tseung Kwan O (Fig. 2).

The fractions of different land cover tiles within a grid are required input parameters for models adopting a tiling/mosaic approach. Based on the detailed surface cover map (Fig. 2), the 'sea tile' and 'inland water tile' (Table 1) are obtained by simply aggregating the sea and inland water surface covers, respectively (Fig. 3a, b). The delimitation of the 'nature tile' and 'urban tile', however, is less trivial since it is related to a somewhat arbitrary decision on which part of the vegetation cover directly interacts with the buildings (urban vegetation) and which part does less/not. As Best and Grimmond (2015) pointed out, urban vegetation plays an important role in influencing the sensible and latent heat fluxes, as well as the radiative and dynamic processes within an urban street

canyon. Therefore, one needs to discriminate in a model grid the proportion of vegetation that should be considered by the UCM from the rest which is treated as purely rural. A threshold established by Bernard (2018) using the ratio between building surface cover and natural surface covers (low/sparse vegetation, high/dense vegetation, bare soil, rock, marsh/mudflat) is employed to determine the 'urban tile' fraction in a grid. For grids with much fewer buildings than vegetation (ratio of building over natural surface cover ≤ 0.02), the 'urban tile' is assumed to be composed of the building surface fraction and impervious (road, pavement, other urban surface covers) surface fraction, as well as a proportion of the natural covers which is twice as much as the latter; whereas for grids with a considerable building fraction (ratio of building over natural surface cover > 0.02), the 'urban tile' contains all

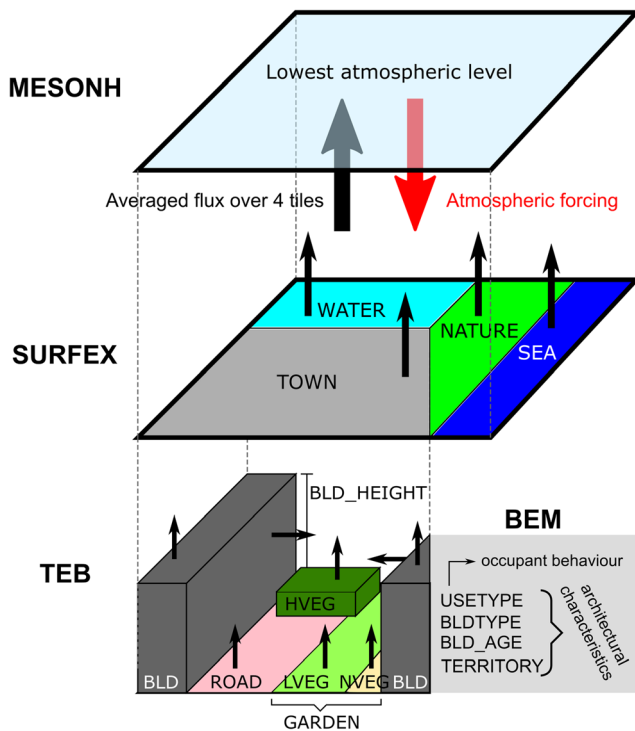


Fig. 1 An example of the hierarchy and types of different model input parameters required for urban climate simulations using the MesoNH-SURFEX-TEB-BEM coupling. Arrows show the energy fluxes from the different surfaces. TOWN, WATER, NATURE, and SEA are land cover tiles within a model grid; within the UCM employed for the TOWN tile, BLD is building surface fraction, ROAD is impervious surface fraction, GARDEN is pervious surface fraction (further separated into low vegetation (LVEG) and bare soil (NVEG)), HVEG is high vegetation fraction above ground, BLD_HEIGHT is the average building height; USETYPE, BLDTYPE, BLD_AGE, and TERRITORY are identifier parameters for inferring architectural characteristics and occupant behaviour of representative buildings

natural surface covers present in the same grid. Clearly, this method involves the subjective judgement of the model user, but it has proved to reasonably smoothen the transitions at urban-rural interfaces (Bernard 2018). Resultant maps are displayed in Fig. 3 for the ROI.

3.3 Urban surface covers and morphological parameters

As described in Section 2, the fractions of building, impervious, and pervious surfaces need to be further defined for the grids with an ‘urban tile’ to be modelled by an UCM. For the maps obtained for the ROI in Hong Kong (Fig. 4), impervious surfaces comprise Road, Pavement, Other urban, and Rock surface covers, while pervious surfaces comprise low/sparse vegetation, high/dense vegetation, bare soil, and marsh/mudflat surface covers. With recent model developments, some UCMs are able to explicitly represent trees in a street canyon and their shading effects (Redon et al. 2017). Hence, a

separate above-ground layer with the amount of high/dense vegetation is presented in Fig. 4d.

There is generally a need for three input parameters relating to building geometry in UCMs: one defining the height of buildings, one providing the aerodynamic roughness length, and one describing the canyon geometry or vertical wall surfaces. For the case of Hong Kong, the average (arithmetic) building height for each 100-m grid (Fig. 5a) is calculated from the height information obtained from the Lands Department. A simple rule-of-thumb approach is then taken to approximate the aerodynamic roughness length as one-tenth of the average building height (Grimmond and Oke 1999). To maximise land use and enhance space connectivity, volumetric developments, such as podium-and-tower structures and agglomerations of building blocks that are not aligned with the streets, emerged in Hong Kong since the change in Building Regulations in the 1970s (Shelton et al. 2011). Such urban configurations make it difficult to define the street orientation and width, and thus the average canyon aspect ratio. Therefore, the wall density (Fig. 5b) is employed to more accurately describe the 3D geometry of urban areas in Hong Kong. It is obtained by summing all the building/podium outlines multiplied by their respective building/podium heights within each grid and dividing it by the area of the ‘urban tile’. Grids with high wall densities in the old urban cores on both sides of the Victoria Harbour are likely to resemble areas with narrow and deep street canyons. Also presented are maps zooming in on the Kowloon Peninsula and showing the building fraction at different height levels (Fig. 6) which may be used by multi-layer UCMs. They provide a more realistic representation of the complex built environment of Hong Kong and are able to highlight the high ground coverage by podiums in the lower levels of the urban canyon (Fig. 6a, b).

3.4 Uncertainties of the urban database

Although the aim here is to construct a refined surface database, especially for urban areas, that is as accurate as possible, certain limitations need to be noted when using this database. First, there may be a slight mismatch in time for the different layers of information due to data availability. Data for sites with on-going construction, redevelopment, or reclamation are prone to be erroneous or missing. Nevertheless, this database is able to represent the realistic urban environment of Hong Kong for mesoscale urban climate simulations. Secondly, the large number of buildings, great variation in building heights, and hilly terrain all add to the challenges of attaining accurate building heights. The building shapefiles obtained from the Lands Department contain heights of building/podium tops and bases, with reference to the mean sea level, collected from a combination of sources such as topographic surveys, building plans, and photogrammetry.

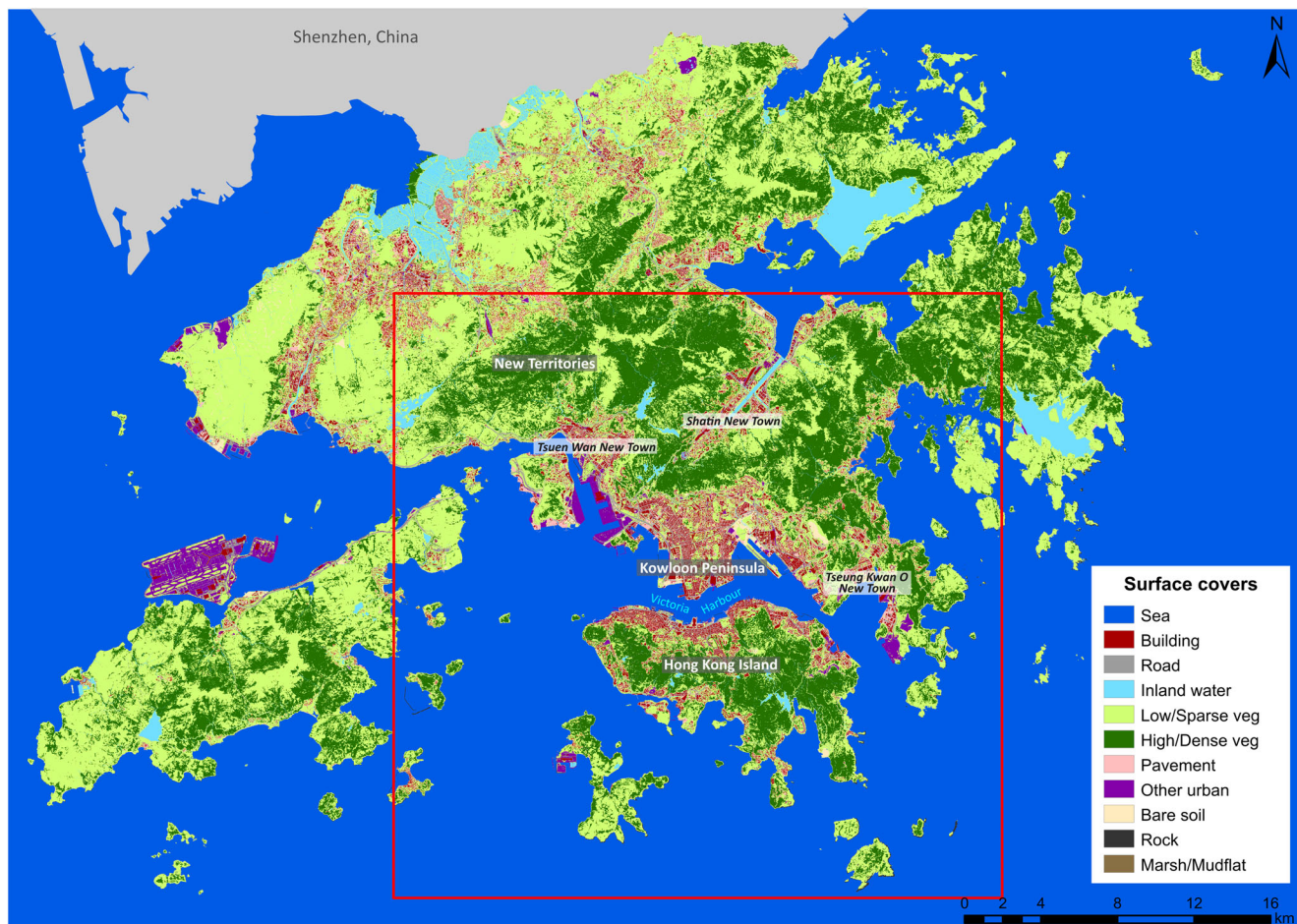


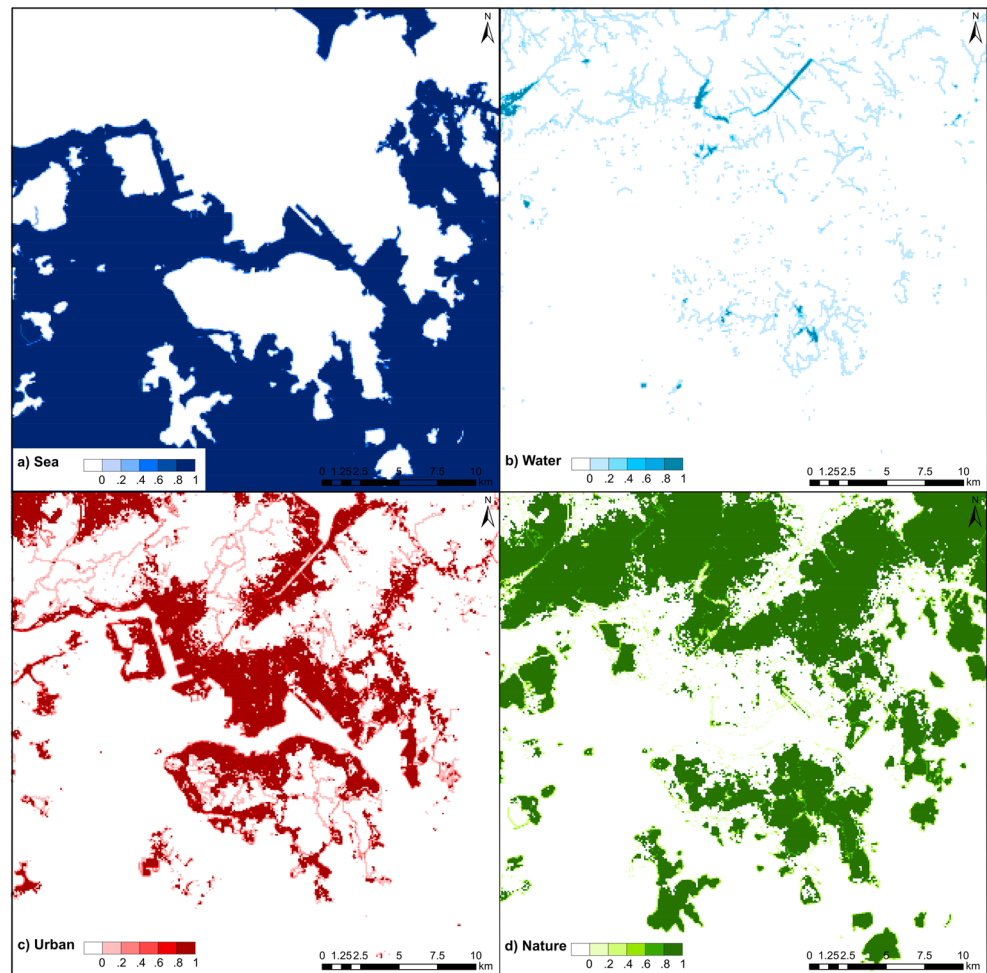
Fig. 2 Detailed surface covers of Hong Kong at 1-m spatial resolution. The red box is the region of interest (ROI) shown in Figs. 3, 4, 5, and 7

Some discrepancy in building/podium heights have been identified for built structures on steep slopes, and some buildings in remote rural areas do not have height information. As a result, these buildings and podiums with erroneous or missing (around 3% of all buildings/podiums) are assigned with arbitrary heights of 3 m (corresponding to around 1 storey) and 1 m, respectively. Moreover, all buildings and podiums are assumed to have a single height and walls perpendicular to the ground when calculating the wall density, since details of the building structure design (e.g. slanting facades, terraced building, tapered structures) are too fine to be considered by a UCM. Thirdly, since there are no publicly available administrative databases for urban vegetation and street trees, information on vegetation density and extent can only be roughly inferred from the NDVI of satellite images. The spatial resolution is therefore limited to 10 m for vegetated surface covers. This may also explain the low ‘high vegetation’ cover for most ‘urban tiles’ in Hong Kong.

A more fundamental uncertainty relevant to the urban climate modelling of Hong Kong is the representation of the urban roughness. In the current database, the aerodynamic roughness length has been calculated as one-tenth of the

average building height, which implies that it represents that of the whole urban canopy. This choice requires the first level of the atmospheric model to be placed at the top of the urban roughness sublayer (with a typical thickness of two to five times the average building height, which translates to more than 100 m above-ground level in most urban districts in Hong Kong) in which the individual buildings directly influence the wind field (Roth 2000). Furthermore, the Monin-Obukhov Similarity Theory employed for the calculation of the surface fluxes assumes horizontal homogeneity of the urban morphology. This is not the case in Hong Kong where isolated skyscrapers, dense high-rise districts, urban parks, forests, and the sea can be found in close proximity to each other. For these reasons, a different modelling approach, already introduced by Martilli et al. (2002) and Chen et al. (2011), should be employed for a complex high-rise city like Hong Kong: the urban canopy immersed in the atmospheric model and the effect of the vertical walls on the wind velocity represented with a drag force that may influence multiple levels of the atmospheric model. With this approach, it is not required anymore to define a roughness length representative for the whole canopy. Instead, the momentum, heat, and

Fig. 3 Maps at 100 m spatial resolution of the **a** sea, **b** inland water, **c** urban, and **d** nature tile fractions for the ROI in Hong Kong



moisture exchanges are calculated with the specific aerodynamic roughness length of different urban facets like roofs, walls, road, and low urban vegetation. Nevertheless, the estimation of a bulk canopy roughness by simple methods such as the one used in this study could be helpful for comparison purposes or for UCMs adopting a standard single-layer modelling approach.

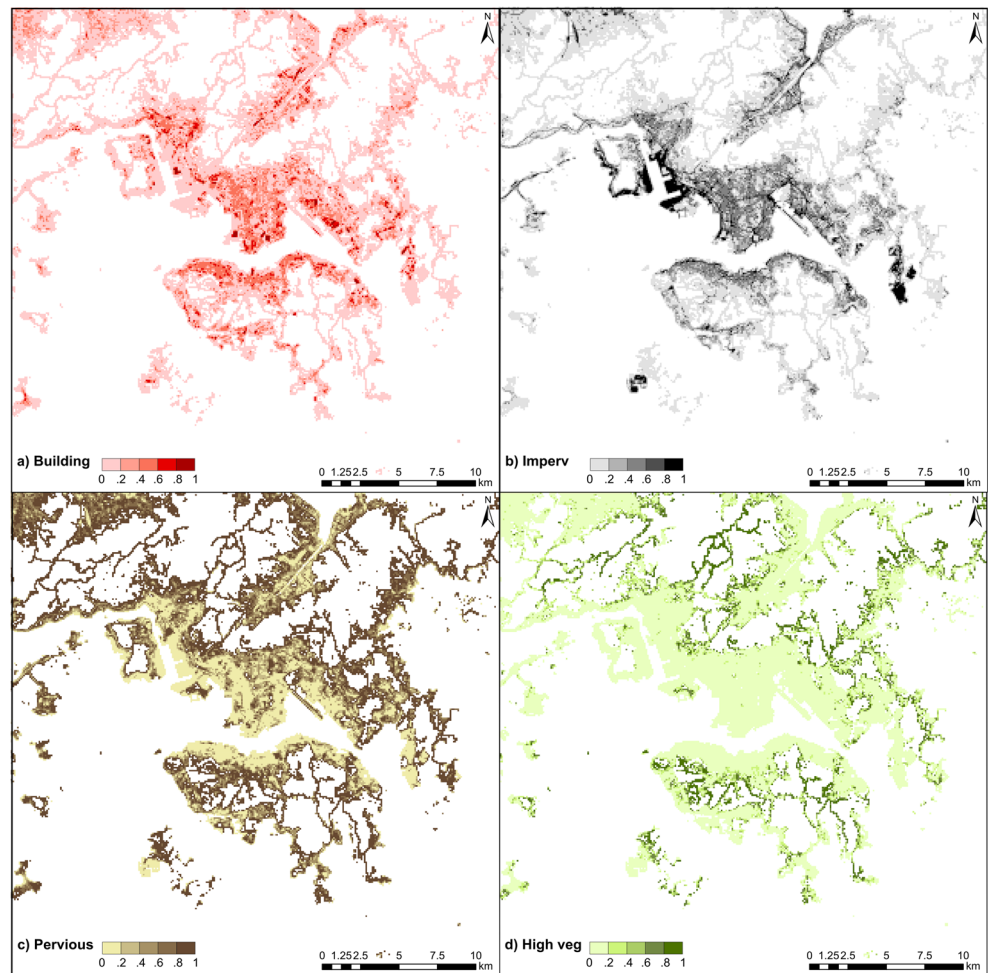
4 Definition of representative buildings for Hong Kong

4.1 Defining building archetypes for Hong Kong

Though detailed data on the footprint and heights of buildings in Hong Kong are available (Section 3), they do not provide any indication on the building architectural characteristics. Learning from the experience of French researchers on building construction practices in France, information on construction materials and occupant behaviour may be inferred from the building type, function, age, and geographic location (Tornay et al. 2017). After reviewing the literature (e.g.

Jaillon and Poon 2009; Shelton et al. 2011; Wong 2014) and seeking expert advice from architects (T. Ip, personal communication, March 29, 2018), it is found that this approach may not be readily applicable to the urban settings of Hong Kong since the majority of wall and roof materials do not change significantly with building age and location, due to Hong Kong's relatively short urbanisation history and the irrelevance of natural materials (e.g. stones) for the construction industry. Hence, there exist less building archetypes in Hong Kong than in France or other European/American countries. A total of 18 representative building archetypes are therefore defined, mainly distinguished by building type and function (Table 2). Some archetypes with largely similar building architectural characteristics and occupancy schedules (e.g. Mid-rise/Village House and Private Housing, School and University) may be merged upon subsequent sensitivity tests. Careful attention has been paid to differentiate the public and private housing, since a change in building architecture, facade design, and podium scale can be observed over time for the latter but not the former (see Fig. 7 in Masson et al. 2020). There could also be a correlation with demographic factors of occupants as residents of the public housing are often of an

Fig. 4 Maps at 100-m spatial resolution of the **a** building, **b** impervious surface, **c** pervious surface, and **d** high vegetation (above surface) fractions for the ‘urban’ grids within the ROI in Hong Kong. Note that these surface fractions are calculated taking the full grid area as the base, but may need to be converted as a fraction of only the ‘urban tile’ depending on model specifications (e.g. a building fraction of 0.2 within a grid where 0.8 of it is ‘urban’ can be translated to a building fraction of 0.25 within the ‘urban tile’)



older age and lower income level than those of the private housing. Some major differences in building architectural

characteristics between different archetypes are presented in Table 2 and will be further discussed in Section 4.2. A detailed

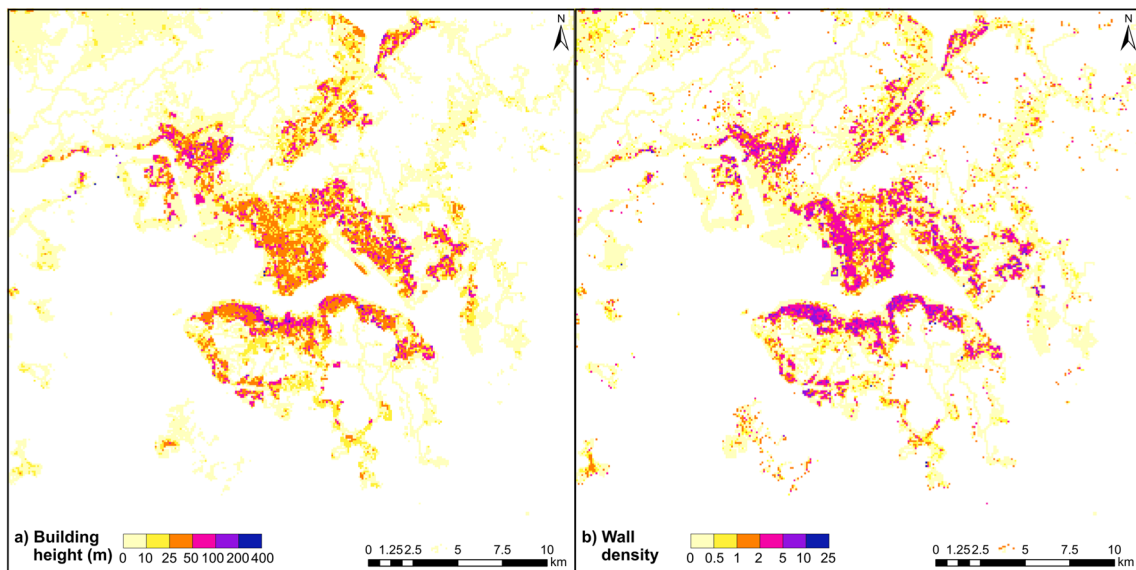


Fig. 5 Maps at 100-m spatial resolution showing the **a** average (arithmetic) building height and **b** wall density for the ‘urban’ grids within the ROI in Hong Kong

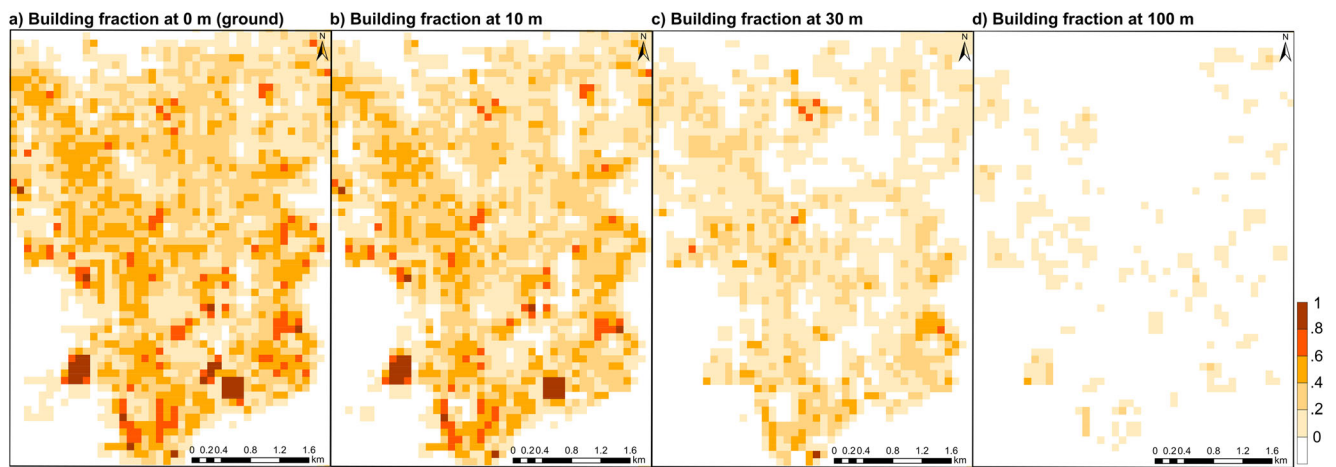


Fig. 6 Maps at 100-m spatial resolution showing the building fraction for the ‘urban’ grids in Kowloon Peninsula at **a** 0 m, **b** 10 m, **c** 30 m, and **d** 100 m above ground

factsheet for each building archetype is provided in the Supplementary Material.

After the building archetypes have been defined, a high-resolution map of the dominant archetype needs to be derived. A spatial resolution of 100 m is chosen such that the building archetypes are known at a higher resolution than the typical resolution of mesoscale urban climate models (250 m to 1 km). There is no existing database on building types and functions at building scale in Hong Kong. The Outline Zoning Plans (OZPs) published by the Town Planning Board (HKPlanD 2019) may serve as a reference on the permitted land use(s) at the street block scale, but the zoning approach is ill-suited for urban climate simulation purposes. For example, buildings may vary greatly in terms of material, facade design, as well as use within a zone for “comprehensive development area” or “other specified uses”. The OpenStreetMap (Haklay and Weber 2008) contains useful crowdsourced data on buildings, especially those with “government, institutional, and community” (GIC) uses, but a large number of building blocks are unfortunately missing in the areas with less public interest in Hong Kong. Due to the inconsistencies among various data sources, it is found more appropriate to adopt a manual approach based on field survey and expert knowledge to obtain the building types and functions for the entire territory. Building archetypes are mapped in a GIS by integrating available online resources, undertaking field surveys, and referring to satellite and Google Street View images. Figure 7 shows the dominant building archetype in terms of habitable floor area at 100-m resolution. Village houses and informal infrastructures are scattered extensively in the suburban areas, and they form the two most frequently occurring building archetypes in the ROI. The third most common building archetype is GIC. Commercial skyscrapers concentrate on the two sides of the Victoria Harbour, while industrial activities can be mainly found in Kwai Tsing, Kwun Tong, Fo Tan, and Tseung Kwan O. Around 40% of buildings within the ROI are

residential, with a public to private housing ratio of around 1:1.5, agreeing with government statistics (HKPlanD 2019).

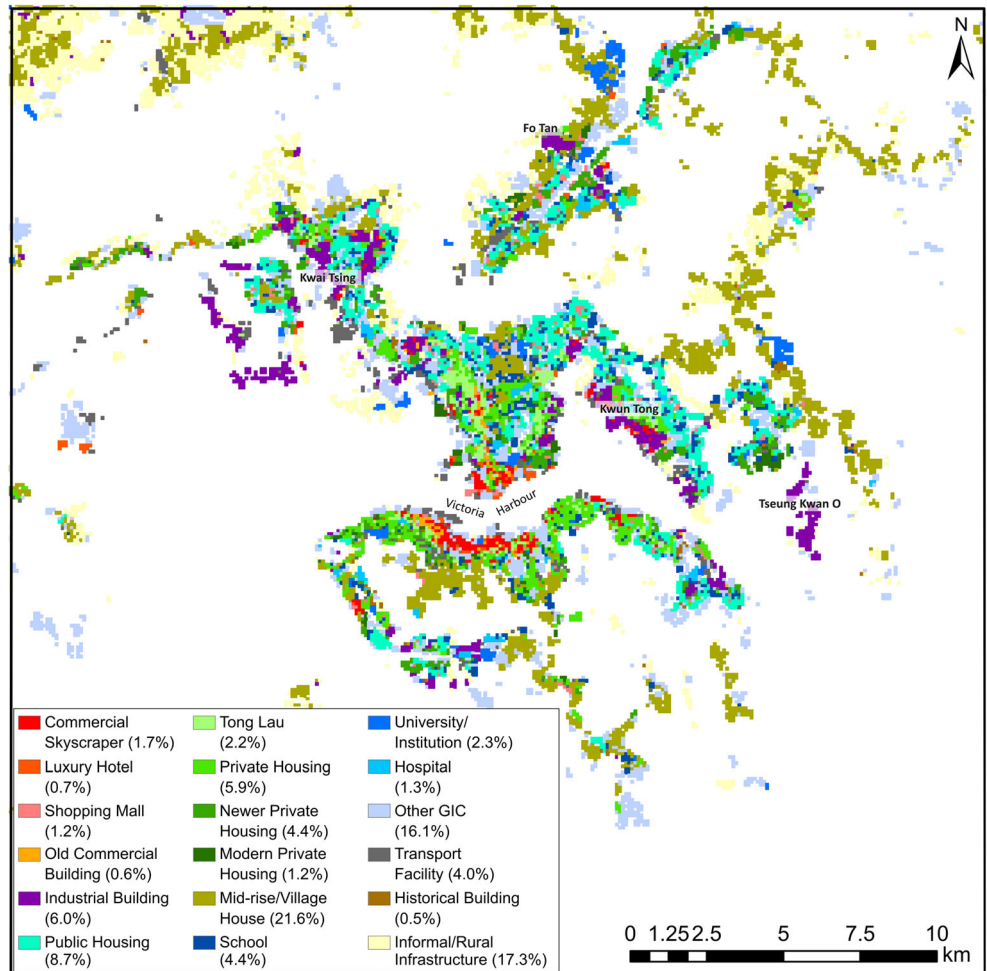
4.2 Building architectural characteristics

Information on the architectural characteristics of buildings in Hong Kong has been collected by consulting practitioners in the building industry (W.H. Cheung, personal communication, March 20, 2018, T. Ip, personal communication, March 29, 2018), reviewing the relevant building codes and guidelines (e.g. HKEMSD 2018), and making reference to building simulation studies (e.g. Kwok et al. 2017 and references therein). Since the early 20th century when high-density urban development began in the form of tenement houses (Tong Lau), concrete has been the dominant structural material for most buildings in Hong Kong, except for Commercial Skyscrapers which commonly adopt a structural system with a steel skeletal frame and glass curtain walls (Ali and Moon 2007). To improve quality control, shorten construction time, and reduce on-site construction waste, the use of prefabricated concrete component blocks for residential buildings has gained popularity in both the public and private sectors (Jaillon and Poon 2009), resulting in relatively standardised building forms. Nevertheless, some trends in facade design can be observed as driven by changes in building codes through the years (Wong 2014). An example is the emergence of “bay windows” between 1980 and 2012 (in Newer Private Housing) due to government policy on its exemption from the restriction of “gross floor area” (HKBD 2014a). Extra care has been taken to capture the differences in glazing type and window-to-wall ratios when defining the 18 building archetypes (Table 2) because previous studies (e.g. Lam et al. 2005) have shown that solar heat gain through windows contributes the most to the total building envelope heat gain, and thus cooling energy demands. To regulate the energy performances of buildings, the government introduced

Table 2 Selected building architectural characteristics of the 18 building archetypes defined for Hong Kong. Refer to the Appendix for more detailed information on each building archetype and the physical and thermal properties of different building materials to be used by an UCM

Building archetype	Window type	Glazing ratio (%)	Wall main material	Wall insulation	Roof material	Airtightness (air exchange rate [1/h] at 50 Pa)	Mechanical ventilation	Air exchange rate due to mech. vent. (1/h)	Occupant schedule
Commercial skyscraper (CS)	Double glazing	80	Metal frame	Yes	Reinforced concrete	4	Yes	0.7	Office
Luxury hotel (LH)	Double glazing	50	Reinforced concrete	Yes	Reinforced concrete	4	Yes	0.6	24/7
Shopping mall (SM)	Tinted glass	30	Reinforced concrete	No	Reinforced concrete	4	Yes	0.7	Commerce
Old commercial building (OC)	Single glazing	30	Reinforced concrete	No	Reinforced concrete	4	Yes	0.7	Commerce
Industrial building (IB)	Single glazing	30	Reinforced concrete	No	Reinforced concrete	4	Yes	0.3	Industrial
Public housing (PU)	Single glazing	20	Reinforced concrete	No	Reinforced concrete	4	Yes	0.3	Residential
Tong Lau (TL)	Single glazing	35	Concrete	No	Reinforced concrete	4	Yes	0.3	Residential
Private housing (PR)	Single glazing	25	Reinforced concrete	No	Reinforced concrete	4	Yes	0.3	Residential
Newer private housing (NPR)	Tinted glass	35	Reinforced concrete	No	Reinforced concrete	4	Yes	0.3	Residential
Modern private housing (MPR)	Double glazing	60	Reinforced concrete	No	Reinforced concrete	4	Yes	0.3	Residential
Mid-rise/village house (VH)	Tinted glass	40	Reinforced concrete	No	Reinforced concrete	4	Yes	0.3	Residential
School (SC)	Single glazing	30	Reinforced concrete	No	Reinforced concrete	4	Yes	1.8	School
University/institution (UI)	Tinted glass	40	Reinforced concrete	No	Reinforced concrete	4	Yes	1.8	University
Hospital (HO)	Tinted glass	30	Reinforced concrete	No	Reinforced concrete	4	Yes	2.0	24/7
Other GIC (GIC)	Single glazing	25	Reinforced concrete	No	Reinforced concrete	4	Yes	1.2	GIC
Transport facility (TF)	Single glazing	10	Reinforced concrete	No	Reinforced concrete	20	No	N/A	24/7
Historical building (HB)	Single glazing	10	Wood	No	Wood	8	No	N/A	24/7
Informal/rural infrastructure (IR)	Single glazing	20	Concrete	No	Corrugated metal	20	No	N/A	24/7

Fig. 7 Dominant building archetype in terms of habitable floor area at a spatial resolution of 100 m within the ROI in Hong Kong. Proportion of grids for each building archetype in the ROI is shown in brackets in the legend



the Overall Thermal Transfer Value (OTTV) standard for commercial buildings and hotels in 1995 (HKBD 1995) and the subsequent Residential Thermal Transfer Value (RTTV) for residential buildings in 2015 (HKBD 2014b), in which typical wall and roof structures with their corresponding material properties are provided for reference. Due to the subtropical climate of Hong Kong, another architectural feature to note for local buildings is the infrequent use of wall insulation and double glazing. As a result, building indoor conditions or energy demand due to HVAC are highly responsive to outdoor temperature variations. Lastly, the mechanical ventilation rates are calculated based on the typical occupant density, floor-to-floor height, and minimum volume of outdoor air per person provided in government guidelines (HKEMSD 2007).

4.3 Parameters relating to building energy usage

Energy consumption in buildings is affected by the design of the building envelope, the energy efficiency of the heating, and ventilation and air-conditioning (HVAC) systems, as well as the energy usage patterns of occupants or machinery. In this study, representative occupant schedules are set for building

archetypes with different functions according to past questionnaire surveys (e.g. Chen and Lee 2010), monitoring studies (e.g. Lam et al. 2003), and the local knowledge and experience of the authors. The schedules are set differently for weekdays and weekends to consider a typical weekly cycle (Fig. 8). Note that some schedules are specific for the case of Hong Kong, such as the partial occupancy of educational buildings in the evenings and during weekends when extra-curricular activities take place. These schedules control the operation of air-conditioning and internal heat release due to lighting, equipment load, and warm water etc. Appropriate indoor set point temperatures and target relative humidity for when the building is occupied and vacant are also specified. For example, the indoor design temperature in occupied commercial buildings is set to 22–23 °C (Wong et al. 2008; Jia and Lee 2018), while it is set to 25 °C for other dwellings since this is the design temperature recommended by the government. However, with this choice, it is assumed that inhabitants comply with the government recommendation, which might not be the case.

The QF contributes significantly to the urban SEB, but it is not readily measured. One of the methods to estimate the anthropogenic emissions from the building sector is to rely

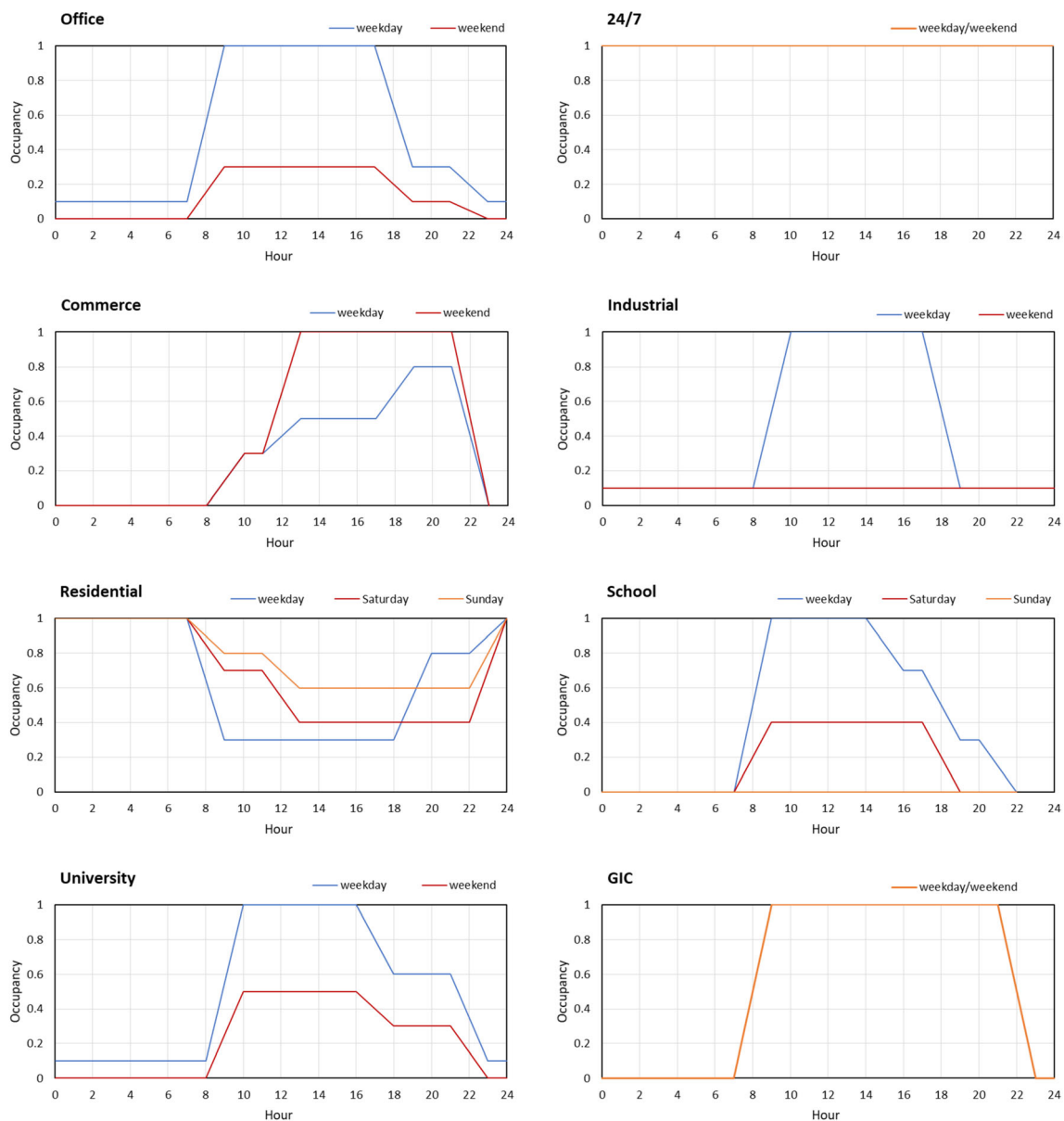


Fig. 8 Representative occupant schedules for building archetypes with different building functions

on building energy models. Sailor (2011) pointed out the strong spatio-temporal variability of the QF and suggested a prototypical approach for building models so that realism and practicality can be balanced. Therefore, the information on occupant behaviour and energy use patterns for different building archetypes provided here would allow the accurate estimation of QF for use in urban climate simulations at the mesoscale.

4.4 Uncertainties of the building archetype database

Some specific limitations to the building archetype database and classification approach in describing the urban environment of Hong Kong are noted. First, there needs to be a trade-

off between accuracy and simplicity. On the one hand, the building archetypes should be able to capture the different architectural characteristics and occupant behaviour that influence the urban SEB; on the other hand, the number of building archetypes needs to be limited. As such, certain variations within a single building archetype have to be neglected. For example, the archetype Other GIC may contain buildings from community halls and indoor sports grounds, to police and fire stations, or even museums and rubbish collection centres. Another example is the Tong Lau, which commonly hosts commercial activities on the ground/lower floor(s) and accommodates relatively low-income residents in subdivided flats above. The current occupant schedule associated with the Tong Lau does not consider this mix of building use. Since the

proposed building classification approach aims to provide refined urban surface input data for mesoscale atmospheric models, the 18 building archetypes currently defined are deemed reasonable. Sensitivity tests may be conducted for different models to further refine and simplify the building archetype classification. Secondly, podiums have not been included in the building archetype classification. They are commonly built beneath building towers of private housing estates. They cause uncertainty in the building archetype database because of their variable architectural design and functions (e.g. carparks, recreational facilities, shopping malls). Another uncertainty in the classification comes from the lack of precise information to differentiate village houses and informal infrastructures, especially in rural areas in the New Territories. Google Street View images, which serve as an important data source for the building classification, are often unavailable in these areas due to the prohibited vehicle access in private roads and footpaths.

4.5 Global applicability of this building archetype approach

So far, this building archetype approach has been adopted in France (Tornay et al. 2017) and Hong Kong (ongoing) to provide detailed input parameters related to building architecture and occupant behaviour in a mesoscale atmospheric model. Considerable differences can already be observed in these two places. The total number of building archetypes in Hong Kong is much lower than in France since there are no differences in archetypes due to the geographical location and thermal regulation periods (building age). In France, residential buildings are subclassified into individual and collective housing, but this concept is not applicable in Hong Kong since nearly all housing is collective. Instead, residential buildings are subclassified into Public housing, Private housing, Tong Lau, and Village House. Historical buildings in France may refer to castles or churches left from medieval times, whereas in Hong Kong, the oldest buildings mostly date back only to the early nineteenth century. Therefore, if a similar building archetype approach is to be applied to other countries/cities in the world, it may need to be locally adapted depending on the location's urban development history, climate, demographics, and culture. In countries/cities with serious income disparity, differences in building design and occupant behaviour may also be a function of the local or household income level. Cities with a dire need to combat climate change are often located in developing countries with tropical/subtropical climates, many of which are in the state of rapid urbanisation. In such case, the number of building archetypes may be reduced because it is likely that the use of insulation does not need to be considered, and the buildings do not differ much in construction materials and architectural design.

Another concern is on data availability and efficiency of classification. Due to the absence of existing data layers which may infer the architectural characteristics and occupant behaviour of buildings in Hong Kong, the workload to manually map building archetypes is immense even with the help of more than 15 student helpers. In France, a supervised classification of building types was complemented by a database compiled by an architect's expertise approach. Currently, building architectural information with international coverage collected from machine learning and crowdsourcing approaches are becoming available as part of the WUDAPT initiative (Ching et al. 2019). The Google Maps Platform with Places API services and the Popular Times feature may also be useful for obtaining data on building functions and human behaviour in future works.

5 Development and evaluation of locally adapted urban morphological parameter ranges per LCZ

5.1 LCZ map of Hong Kong

When a detailed urban morphology database as presented in Section 3 is not available, a LCZ map, obtainable by both GIS and freely-available remote sensing methods, may be used to provide a categorical description of the geometric and surface cover properties of cities (Ching et al. 2019). Though initially developed to provide an international standard for the documentation of measurement sites in UHI studies, the set of parameters associated with each LCZ, especially for the ten urban classes (LCZs 1–10), is able to provide a reference for the input parameters typically required in urban climate modelling. A geospatial analysis is conducted on the ROI to extract from the refined urban database the values of UCM input parameters for each LCZ in Hong Kong and to examine how these values compare with generic ranges in the LCZ look-up table proposed by Stewart and Oke (2012); SO12 ranges).

The LCZ map of Hong Kong used in this study is derived by Wang et al. (2018a) based on real building and land use data of 2009. There is a mismatch of time frame between the LCZ map and the refined urban database, but any errors that may have arisen should be minor as there have not been major developments at the pixels of urban LCZ classes within the ROI in the past decade, except for the ongoing projects at West Kowloon Cultural District and the former Kai Tak airport. Within the ROI, the predominance of LCZs 1 (compact high-rise; 21%) and 4 (open high-rise; 31%) reflects the prevalence of high-rise buildings in Hong Kong. The village houses scattered in the urban-rural interfaces are mostly classified as LCZ 9 (sparsely built; 16%). Note that at the spatial resolution of 100 m, no pixels have been identified as LCZ 7 since

single-storey buildings constructed out of lightweight materials, such as wood, thatch, and corrugated metal, are rare in Hong Kong. It should also be noted that the user's accuracies of the map used (i.e. the number of correctly classified pixels over the total number of actual validation pixels of a certain LCZ class) for LCZs 2 (compact mid-rise), 6 (open low-rise), and, in particular, 8 (large low-rise) are relatively low and thus need to be analysed with caution (Wang et al. 2018a).

5.2 Locally adapted parameter ranges per LCZ

Since LCZ maps are now readily obtainable for any city agglomeration via remote sensing using the WUDAPT methodology (Ching et al. 2018), it is practical to use LCZ classes and their associated parameter values for the initialisation of UCMs. When detailed urban data is not fully available for a large study area, the use of a locally adapted look-up table to extend the coverage of representative urban data can be considered a good compromise between feasibility and data accuracy. Taking this study as an example, the detailed urban surface cover and morphological parameters (Figs. 4 and 5) can be extrapolated to areas beyond the ROI, including the PRD region which is characterised by similar high-density and high-rise urban settings, by assigning representative parameter values for each LCZ. Table 3 presents the urban morphological parameters for each LCZ adapted to the urban environment of Hong Kong. The mean value of each parameter obtained from the geospatial analysis is taken to be representative of the LCZ in Hong Kong.

5.3 Comparison between the local and generic ranges of LCZ characteristics

The relevance of the generic look-up table proposed by Stewart and Oke (2012) to the urban environment in Hong Kong is examined by comparing the parameter value ranges for different LCZs (Fig. 9). Besides the building, impervious, and pervious surface fractions, the geometric average building height is compared to the height of roughness elements for different LCZs. The geometric average dampens the effects of extreme outliers and is more representative of the average obstacle roughness. Note that the difference between the arithmetic and geometric averages may serve as an indication of the heterogeneity of building heights. The locally representative building surface fractions are largely fitting into the SO12 ranges, except for LCZ 8, for which the building surface fraction is much lower than in SO12. In Hong Kong, LCZ 8 (large low-rise buildings) mostly corresponds to warehouses, wholesale markets, and depots. The buildings themselves usually only occupy a small proportion of the site, surrounded by large paved areas (e.g. car parks, container ports, non-building facilities). The lower building fraction for LCZ 8 may also be due to the shortcomings of the LCZ map. The

local building surface fractions of LCZs 2 and 3 fall on the lower end of the SO12 ranges. However, such values are already higher than the building surface fractions of LCZs 2 and 3 in Dublin (Alexander et al. 2015) by a factor of 1.3 and 1.8, respectively, showing an example of the large variation in surface cover fractions that may exist in different cities. Thanks to the small urban parks and roadside greenery that penetrate the densely-developed urban cores of Hong Kong, compact LCZs (LCZs 1, 2, 3) have relatively high pervious surface fractions and low impervious surface fractions. Although the local pervious surface fractions of open LCZs (LCZs 4, 5, 6) are within the SO12 ranges, they are 10–20% lower than that of open LCZs in Toulouse (Hidalgo et al. 2019). This confirms the high variability in surface characteristics across urban settings in cities worldwide and highlights the importance of being cautious with simulation results when using SO12 ranges since they may not reflect the local urban morphology. As expected, the average building height of most LCZs complies with the SO12 ranges because building height thresholds according to the SO12 ranges have been used for the GIS-mapping of LCZs 1 to 6 in Hong Kong. The large number of high outliers for LCZs 1 and 4 reflect the prevalence of skyscrapers in the heterogeneous and high-rise built environment of Hong Kong. However, these extremely tall buildings cannot be distinguished from other tall buildings using the current LCZ scheme which groups all buildings with heights greater than 25 m into a single class. This limitation will be further discussed in the next section.

5.4 Limitations of the LCZ scheme for a complex high-rise city

Due to the lack of flat land and the large population, urban development in Hong Kong has long taken the vertical expansion approach. Therefore, Hong Kong is characterised by a large number of very high-rise buildings, which directly impact the circulation and thermodynamics of the lower atmosphere (due to the drag force, heat, and moisture fluxes caused by buildings). It is found that the high outliers for LCZs 1 and 4 (Fig. 9d) can correspond to buildings of various functions, including Commercial Skyscrapers, Industrial Buildings, Public Housing, and Modern Private Housing (not shown). The heterogeneous built environment in Hong Kong makes it challenging to establish potential links between LCZs (urban form) and building functions, as opposed to some western cities, where distinct areas composed of similar urban form and functions can often be identified. For instance, typical US urban settings may be described as follows: tall commercial buildings (LCZ 1) dominate in the city centre, surrounded by apartment buildings that are more widely spaced (LCZ 4), with large low-rise commercial or industrial buildings (LCZ 8 or 10), and homogeneous low-rise houses (LCZ 6) built in the suburbs. However, in Hong Kong, a majority of building

Table 3 Surface cover and morphological parameters per LCZ representative of the Hong Kong urban environment

Local climate zone (LCZ)	No. of pixels, proportion (%)	Building surface fraction (-)	Impervious surface fraction (-)	Pervious surface fraction (-)	Average building height(<i>m</i>)		Wall density (-)
					Arithmetic	Geometric	
LCZ 1 Compact high-rise	1602 (21%)	0.483	0.382	0.126	42.9	32.0	3.33
LCZ 2 Compact mid-rise	384 (5%)	0.422	0.329	0.232	21.9	17.7	1.41
LCZ 3 Compact low-rise	87 (1%)	0.413	0.211	0.314	9.2	8.1	0.82
LCZ 4 Open high-rise	2303 (31%)	0.275	0.372	0.337	43.8	33.7	2.23
LCZ 5 Open mid-rise	946 (13%)	0.271	0.333	0.364	20.4	16.6	1.08
LCZ 6 Open low-rise	678 (9%)	0.242	0.193	0.525	8.3	7.3	0.58
LCZ 8 Large low-rise	193 (3%)	0.097	0.523	0.238	14.1	12.0	0.42
LCZ 9 Sparsely built	1185 (16%)	0.148	0.153	0.658	7.0	6.3	0.38
LCZ 10 Heavy industry	124 (2%)	0.348	0.344	0.274	28.3	23.2	1.52

archetypes fall into the high-rise LCZ classes (Fig. 10), resulting in a complex mix of building types and functions within the same LCZ class (Table 4).

Table 4 summarises the results obtained from a further analysis to quantify the proportion of the 18 building archetypes (in terms of habitable floor area) found within each urban LCZ in Hong Kong. As mentioned in Section 2, some models make use of the same urban categories to assign both the morphological and building energy-related input parameters from look-up tables. This approach has worked reasonably well in cities with less complex and more homogeneous urban settings (e.g. Phoenix (Shaffer et al. 2015), Berlin (Jänicke et al. 2016), Oklahoma City (Nemunaitis-Berry et al. 2017)), where three urban categories, namely commercial/industrial, high-intensity residential, and low-intensity residential, can sufficiently represent the variation in urban morphology as well as building architecture/function. However, in Hong Kong, the heterogeneity in building morphology represented by the nine urban LCZ classes does not coincide with the heterogeneity in building archetypes. The diverse built environment would be heavily under-represented if each LCZ was to be matched with only one ‘representative’ building archetype. Taking the two most prevalent LCZs as examples, 81% and 63% of building archetypes occurring in LCZs 1 and 4 could not be accounted for should the characteristics of only the most frequent building archetype be used for model input (Table 4). Hence, by proposing a classification of building archetypes in addition to the LCZs, the description of Hong Kong’s built environment is improved, addressing the inadequacies of the current LCZ scheme in

differentiating buildings of different types and functions, especially for the high-rise classes.

6 Conclusion

With the advancement of ULSMs and the demand for urban climate modelling studies at increasingly fine scales, there is a general need to obtain detailed urban databases that can adequately describe the spatial variability of surface cover, urban morphology, and building function within cities. In this study, a refined urban database comprising maps of typical input parameters required by mesoscale urban climate models is constructed for the high-density, high-rise city of Hong Kong. First, a detailed surface cover map (1-m spatial resolution) is produced by compiling data layers from administrative databases, land use maps, and satellite images. The sea, inland water, urban, and nature tile fractions are then obtained by aggregating pixels of respective covers. Within the urban tiles, the fractions of building, impervious and, pervious surfaces are calculated. The average building height and wall density are used to describe the 3D characteristics of the urban environment. To better capture the high building fractions near the ground due to the prevalence of podium-and-tower structures in Hong Kong, the vertical distribution of built density could also be defined for multi-layer UCMs. Nevertheless, due to the multiple data sources, there may be a slight mismatch in time for the different layers of information. Uncertainties in building height for structures

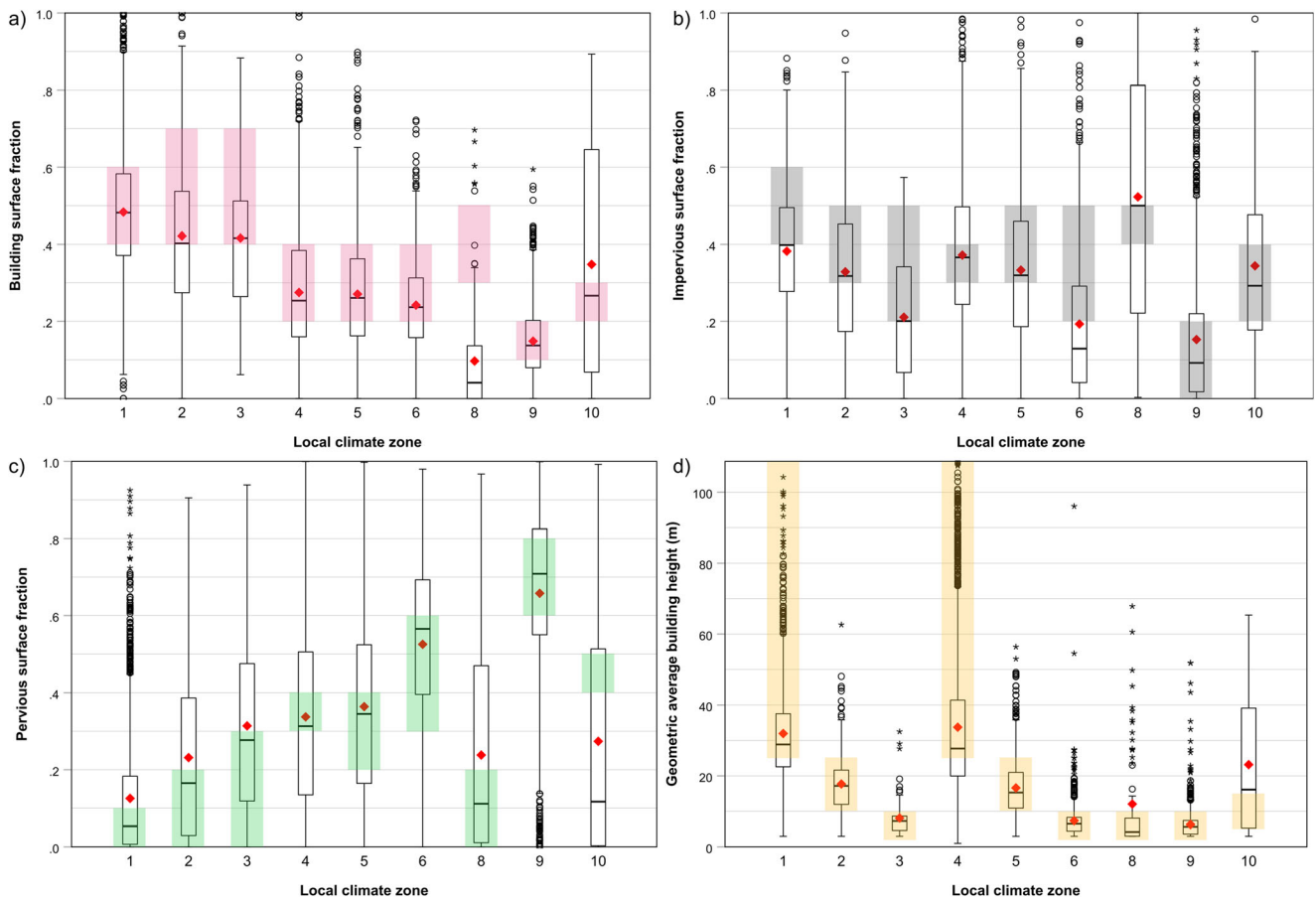


Fig. 9 Comparison between the local (box plots; based on the refined urban dataset of this study) and generic (colour-shaded areas; as proposed by Stewart and Oke 2012) value ranges for **a** building surface fraction, **b** impervious surface fraction, **c** pervious surface fraction, and **d** geometric average building height. Note that 39 outliers with average building height exceeding 100 m are not displayed. Red diamonds show the

mean parameter value for each LCZ; boxes show the median, and the first and third quartiles; whiskers show the highest/lowest value within 1.5 times the interquartile range; circles are outliers that fall above or below 1.5 times the interquartile range; asterisks are extreme outliers that fall above or below 3 times the interquartile range

built on steep slopes and remote locations, as well as the lack on high-resolution data on street trees should also be noted.

In order to differentiate the differences in building architectural characteristics and occupant behaviour that would influence the urban SEB, 18 local building

Fig. 10 The mean geometric average building height of building archetypes within the ROI of Hong Kong. Error bars indicate the 2.5 and 97.5 percentiles. Dashed lines at 10 m and 25 m correspond to the divisions for low-, mid-, and high-rise in the LCZ scheme

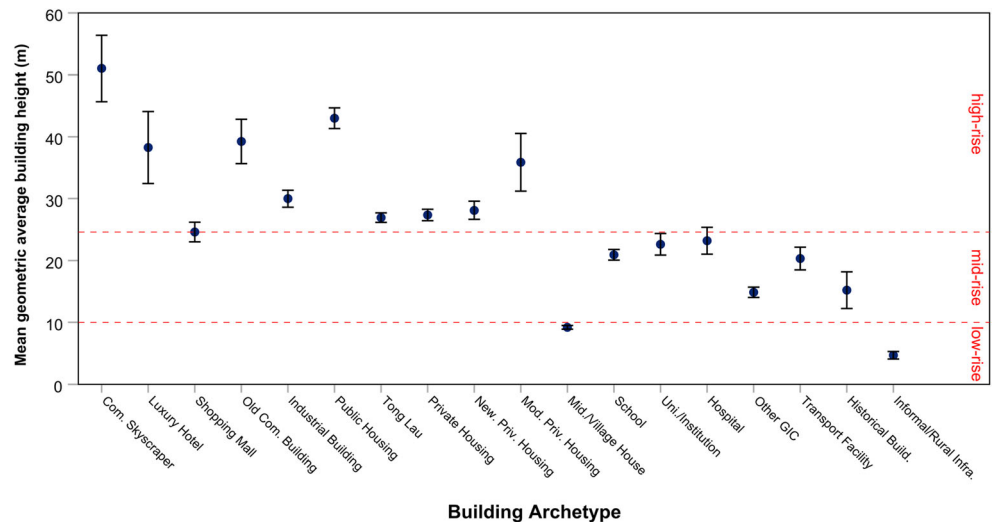


Table 4 The proportion (in terms of habitable floor area) of the 18 building archetypes in each urban LCZ within the ROI of Hong Kong. Bold text highlights the percentage of the most frequent building

archetype and shaded grids show the five most frequent building archetypes for each LCZ. Refer to Table 2 for acronyms of building archetypes

	CS	LH	SM	OC	IB	PU	TL	PR	NPR	MPR	VH	SC	UI	HO	GIC	TF	HB	IR
LCZ1	13.7%	2.6%	3.9%	4.7%	19.5%	4.9%	8.4%	16.4%	14.1%	2.9%	0.4%	1.2%	0.6%	0.9%	2.7%	2.7%	0.3%	0.1%
LCZ2	1.5%	0.1%	4.8%	0.2%	7.7%	11.2%	9.7%	7.6%	11.0%	4.6%	6.4%	3.8%	6.2%	1.9%	10.6%	11.7%	0.3%	0.7%
LCZ3	0.0%	0.0%	1.2%	0.2%	2.4%	0.3%	3.1%	5.8%	0.8%	7.2%	34.5%	0.8%	6.0%	0.0%	17.5%	4.6%	1.7%	13.8%
LCZ4	6.0%	1.3%	3.6%	1.4%	9.2%	36.9%	4.2%	10.6%	8.7%	1.9%	1.1%	3.8%	2.0%	1.6%	4.6%	3.0%	0.2%	0.1%
LCZ5	4.3%	0.4%	2.0%	0.6%	6.4%	8.9%	3.9%	9.9%	8.3%	1.6%	15.9%	12.7%	2.7%	3.4%	11.2%	6.9%	0.5%	0.4%
LCZ6	0.0%	0.0%	1.2%	0.6%	4.6%	3.5%	0.2%	1.1%	1.3%	0.3%	46.8%	4.6%	0.9%	1.6%	14.4%	1.6%	0.8%	16.5%
LCZ8	1.2%	0.0%	0.0%	2.0%	74.4%	5.0%	2.4%	0.0%	0.0%	0.0%	2.6%	0.0%	0.0%	0.2%	3.1%	2.5%	0.0%	6.5%
LCZ9	1.7%	0.9%	0.8%	0.0%	3.9%	4.0%	0.2%	2.1%	1.2%	0.7%	47.2%	2.0%	1.3%	1.8%	11.9%	1.1%	0.3%	19.0%
LCZ10	8.2%	1.0%	2.6%	1.8%	84.3%	1.1%	0.0%	0.0%	0.0%	0.0%	0.1%	0.1%	0.0%	0.0%	0.1%	0.2%	0.0%	0.5%

archetypes are identified based on building type and function. The dominant building archetype in terms of habitable floor area for each 100 m grid is mapped on a GIS with reference to available online resources, field surveys, and local expertise. Though time-consuming, this manual method is deemed more appropriate and feasible for the case of Hong Kong than any automated classifications owing to the lack of existing data layers. Representative values of the construction material properties, glazing ratio, rate of mechanical ventilation, cooling setpoint temperature, etc., as well as occupant schedules are then set for each building archetype with reference to the literature, building regulations, and knowledge of the authors. A few unique features can be noted from the building stock of Hong Kong, including the extensive use of concrete during the city’s rapid urban development, the irrelevance of wall insulation under subtropical climate, and the evolution of window design for private residential buildings. Therefore, if a similar building archetype approach to provide architectural and energy-related

parameters for mesoscale atmospheric models is to be applied to other cities in the world, the number and characteristics of building archetypes should be modified depending on the location’s urban development history, climate, demographics, and culture.

When it is not feasible to obtain detailed maps of urban morphological parameters, a categorical approach is often adopted, making use of readily accessible LCZ maps and a look-up table for corresponding parameter values. To account for the global variation in city characteristics, the use of locally adapted look-up tables should be encouraged. The parameter values representative of the urban environment of Hong Kong largely fall within the generic SO12 ranges, but certain local features can be identified, such as the relatively low impervious surface fractions and high pervious surface fractions for compact LCZs. However, two major limitations of the LCZ scheme in describing heterogeneous, high-rise urban environments such as that of Hong Kong are pointed out: first is its inability to distinguish skyscrapers from other average high-rise buildings and second is the missing link between building

form and building function. City-specific building archetype information, if available, may be used to supplement on the LCZ description.

The novelty of this study lies in the completeness and level of detail (100-m spatial resolution) provided for all typical parameters required for initialising UCMs, with additional information on building architectural characteristics and occupant behaviour and energy-related parameters for representative buildings in BEMs. The workflow has been clearly presented with uncertainties thoroughly discussed such that a similar approach may be adapted and applied to other cities in the world. Further work will be conducted to employ this refined urban database in the mesoscale urban climate simulation of Hong Kong and to test the impact of data precision on the model performance.

Acknowledgments The work is supported by a grant from the PROCORE-France/Hong Kong Joint Research Scheme sponsored by the Research Grants Council and the Consulate General of France in Hong Kong (Reference No. F-CUHK403/18), as well as the Vice-Chancellor's Discretionary Fund of the Chinese University of Hong Kong. The authors would also like to thank all students who have helped with the mapping of building archetypes, as well as practitioners from Sang Hing Construction Company Limited for their advice on building construction materials. The LCZ data used in this study have been developed by Miss Meng Cai and Miss Ran Wang.

Compliance with ethical standards

Conflict of Interest The authors declare that they have no conflict of interest.

References

- Alexander PJ, Mills G, Fealy R (2015) Using LCZ data to run an urban energy balance model. *Urban Clim* 13:14–37
- Ali MM, Moon KS (2007) Structural developments in tall buildings: current trends and future prospects. *Archit Sci Rev* 50(3):205–223
- Allen L, Lindberg F, Grimmond CSB (2011) Global to city scale urban anthropogenic heat flux: model and variability. *Int J Climatol* 31(13):1990–2005
- Avissar R, Pielke RA (1989) A parameterization of heterogeneous land surfaces for atmospheric numerical models and its impact on regional meteorology. *Mon Weather Rev* 117(10):2113–2136
- Bernard M (2018) (In French) Modélisation de la variabilité micro-climatique à l'échelle du quartier, en lien avec l'hétérogénéité paysagère. Master's degree report. 28 pp.
- Best M, Grimmond C (2015) Key conclusions of the first international urban land surface model comparison project. *Bull Am Meteorol Soc* 96(5):805–819
- Bocher E, Petit G, Bernard J, Palominos S (2018) A geoprocessing framework to compute urban indicators: the MApUCE tools chain. *Urban Clim* 24:153–174
- Bonczak B, Kontokosta CE (2019) Large-scale parameterization of 3D building morphology in complex urban landscapes using aerial LiDAR and city administrative data. *Comput Environ Urban Syst* 73:126–142
- Bueno B, Pigeon G, Norford LK, Zibouche K, Marchadier C (2012) Development and evaluation of a building energy model integrated in the TEB scheme. *Geosci Model Dev* 5:433–448
- Chen H, Lee WL (2010) Combined space cooling and water heating system for Hong Kong residences. *Energy Buildings* 42(2):243–250
- Chen F, Kusaka H, Bornstein R, Ching J, Grimmond C, Grossman-Clarke S et al (2011) The integrated WRF/urban modelling system: development, evaluation, and applications to urban environmental problems. *Int J Climatol* 31(2):273–288
- Ching J, Brown M, Burian S, Chen F, Cionco R, Hanna A, Hultgren T, McPherson T, Sailor D, Taha H, Williams D (2009) National urban database and access portal tool. *Bull Am Meteorol Soc* 90(8):1157–1168
- Ching J, Mills G, Bechtel B, See L, Feddema J, Wang X et al (2018) World urban database and access portal tools (WUDAPT), an urban weather, climate and environmental modeling infrastructure for the anthropocene. *Bull Am Meteorol Soc* 2018
- Ching J, Aliaga D, Mills G, Masson V, See L, Neophytou M, Middel A, Baklanov A, Ren C, Ng E, Fung J, Wong M, Huang Y, Martilli A, Brousse O, Stewart I, Zhang X, Shehata A, Miao S, Wang X, Wang W, Yamagata Y, Duarte D, Li Y, Feddema J, Bechtel B, Hidalgo J, Roustan Y, Kim YS, Simon H, Kropp T, Bruse M, Lindberg F, Grimmond S, Demuzure M, Chen F, Li C, Gonzales-Cruz J, Bornstein B, He Q, Tzu-Ping, Hanna A, Erell E, Tapper N, Mall RK, Niyogi D (2019) Pathway using WUDAPT's digital synthetic city tool towards generating urban canopy parameters for multi-scale urban atmospheric modeling. *Urban Clim* 28:100459
- Cox, W. (2019). Demographia world urban areas No. 15th Annual Edition, Demographia.
- De Munck C, Lemonsu A, Bouzouidja R, Masson V, Claverie R (2013) The GREENROOF module (v7. 3) for modelling green roof hydrological and energetic performances within TEB. *Geosci Model Dev* 6(6):1941–1960
- Dong Y, Varquez ACG, Kanda M (2017) Global anthropogenic heat flux database with high spatial resolution. *Atmos Environ* 150:276–294
- Dupont S, Otte TL, Ching JK (2004) Simulation of meteorological fields within and above urban and rural canopies with a mesoscale model. *Bound-Layer Meteorol* 113(1):111–158
- European Space Agency (ESA) (2019) Copernicus open access hub. Retrieved 07/02, 2019, from <https://scihub.copernicus.eu/dhus/#/home>
- Fan H, Sailor DJ (2005) Modeling the impacts of anthropogenic heating on the urban climate of Philadelphia: a comparison of implementations in two PBL schemes. *Atmos Environ* 39(1):73–84
- Garuma GF (2018) Review of urban surface parameterizations for numerical climate models. *Urban Clim* 24:830–851
- Gong F, Zeng Z, Zhang F, Li X, Ng E, Norford LK (2018) Mapping sky, tree, and building view factors of street canyons in a high-density urban environment. *Build Environ* 134:155–167
- Grekousis G, Mountrakis G, Kavouras M (2015) An overview of 21 global and 43 regional land-cover mapping products. *Int J Remote Sens* 36(21):5309–5335
- Grimmond CSB, Oke TR (1999) Aerodynamic properties of urban areas derived from analysis of surface form. *J Appl Meteorol* 38(9):1262–1292
- Grimmond CSB, Blackett M, Best M, Baik J, Belcher S, Beringer J et al (2011) Initial results from phase 2 of the international urban energy balance model comparison. *Int J Climatol* 31(2):244–272
- Haklay M, Weber P (2008) Openstreetmap: user-generated street maps. *IEEE Pervasive Computing* 7(4):12–18
- Hidalgo J, Dumas G, Masson V, Petit G, Bechtel B, Bocher E, Foley M, Schoetter R, Mills G (2019) Comparison between local climate zones maps derived from administrative datasets and satellite observations. *Urban Clim* 27:64–89

- Holt T, Pullen J (2007) Urban canopy modeling of the new york city metropolitan area: a comparison and validation of single-and multi-layer parameterizations. *Mon Weather Rev* 135(5):1906–1930
- Hong Kong Buildings Department (HKBD). (1995). Code of practice for overall thermal transfer value. Hong Kong: BD.
- Hong Kong Buildings Department (HKBD) (2014a) Projections in relation to site coverage and plot ratio - building (planning) regulations 20 & 21 No. APP-19. Hong Kong: BD.
- Hong Kong Buildings Department (HKBD). (2014b). Guidelines on design and construction requirements for energy efficiency of residential buildings. Hong Kong: BD.
- Hong Kong Electrical and Mechanical Services Department (HKEMSD). (2007). Guidelines on performance-based building energy code. Hong Kong: EMSD.
- Hong Kong Electrical and Mechanical Services Department (HKEMSD) (2018) Code of practice for Hong Kong Planning Department (HKPlanD). (2019). Statutory planning portal 2 (SPP2). Retrieved 6/26, 2019, from <https://www1.ozp.tpb.gov.hk/gos/default.aspx?#>
- Hong Kong Planning Department (HKPlanD) (2016) Land utilization in Hong Kong
- Hong Kong Planning Department (HKPlanD) (2019) Land utilization in Hong Kong 2018. Retrieved 8/1, 2019, from https://www.pland.gov.hk/pland_en/info_serv/statistic/landu.html
- Jackson TL, Feddema JJ, Oleson KW, Bonan GB, Bauer JT (2010) Parameterization of urban characteristics for global climate modeling. *Ann Assoc Am Geogr* 100(4):848–865
- Jaillon L, Poon CS (2009) The evolution of prefabricated residential building systems in Hong Kong: a review of the public and the private sector. *Autom Constr* 18(3):239–248
- Jia J, Lee W (2018) The rising energy efficiency of office buildings in Hong Kong. *Energy Buildings* 166:296–304
- Jia G, Xu R, Hu Y, He Y (2015) Multi-scale remote sensing estimates of urban fractions and road widths for regional models. *Clim Chang* 129(3–4):543–554
- Jiang Z, Huete AR, Chen J, Chen Y, Li J, Yan G, Zhang X (2006) Analysis of NDVI and scaled difference vegetation index retrievals of vegetation fraction. *Remote Sens Environ* 101(3):366–378
- Kikegawa Y, Genchi Y, Yoshikado H, Kondo H (2003) Development of a numerical simulation system toward comprehensive assessments of urban warming countermeasures including their impacts upon the urban buildings' energy-demands. *Appl Energy* 76(4):449–466
- Krüger T, Hecht R, Herbrich J, Behnisch M, Oczipka M (2018) Investigating the suitability of sentinel-2 data to derive the urban vegetation structure. *Remote Sensing Technologies and Applications in Urban Environments III*, , 10793. pp. 107930 K.
- Kusaka H, Kondo H, Kikegawa Y, Kimura F (2001) A simple single-layer urban canopy model for atmospheric models: comparison with multi-layer and slab models. *Bound-Layer Meteorol* 101(3):329–358
- Kwok YT, Lai AKL, Lau KK, Chan PW, Lavafpour Y, Ho JCK et al (2017) Thermal comfort and energy performance of public rental housing under typical and near-extreme weather conditions in Hong Kong. *Energy Buildings* 156:390–403
- Lac C, Chaboureau J, Masson V, Pinty J, Tulet P, Escobar J et al (2018) Overview of the meso-NH model version 5.4 and its applications. *Geosci Model Dev* 11:1929–1969
- Lam JC, Li DH, Cheung S (2003) An analysis of electricity end-use in air-conditioned office buildings in Hong Kong. *Build Environ* 38(3):493–498
- Lam JC, Tsang C, Li DH, Cheung S (2005) Residential building envelope heat gain and cooling energy requirements. *Energy* 30(7):933–951
- Lemonsu A, Masson V, Shashua-Bar L, Erell E, Pearlmutter D (2012) Inclusion of vegetation in the town energy balance model for modelling urban green areas. *Geosci Model Dev* 5(6):1377–1393
- Li DH, Yang L, Lam JC (2012) Impact of climate change on energy use in the built environment in different climate zones—a review. *Energy* 42(1):103–112
- Li D, Bou-Zeid E, Barlage M, Chen F, Smith JA (2013) Development and evaluation of a mosaic approach in the WRF-Noah framework. *J Geophys Res Atmos* 118(21):11,918–11,935
- Loga T, Stein B, Diefenbach N (2016) TABULA building typologies in 20 european countries—making energy-related features of residential building stocks comparable. *Energy Buildings* 132:4–12
- Martilli A, Clappier A, Rotach MW (2002) An urban surface exchange parameterisation for mesoscale models. *Bound-Layer Meteorol* 104(2):261–304
- Masson V (2000) A physically-based scheme for the urban energy budget in atmospheric models. *Bound-Layer Meteorol* 94(3):357–397
- Masson V (2006) Urban surface modeling and the meso-scale impact of cities. *Theor Appl Climatol* 84(1–3):35–45
- Masson V, Champeaux J, Chauvin F, Meriguet C, Lacaze R (2003) A global database of land surface parameters at 1-km resolution in meteorological and climate models. *J Clim* 16(9):1261–1282
- Masson V, Le Moigne P, Martin E, Faroux S, Alias A, Alkama R et al (2013) The SURFEXv7. 2 land and ocean surface platform for coupled or offline simulation of earth surface variables and fluxes. *Geosci Model Dev* 6:929–960
- Masson V, Heldens W, Bocher E, Bonhomme M, Bucher B, Burmeister C, de Munck C, Esch T, Hidalgo J, Kanani-Sühring F, Kwok YT, Lemonsu A, Lévy JP, Maronga B, Pavlik D, Petit G, See L, Schoetter R, Tornay N, Votsis A, Zeidler J (2020) City-descriptive input data for urban climate models: model requirements, data sources and challenges. *Urban Clim* 31:100536
- Monaghan AJ, Hu L, Brunsell NA, Barlage M, Wilhelmi OV (2014) Evaluating the impact of urban morphology configurations on the accuracy of urban canopy model temperature simulations with MODIS. *J Geophys Res Atmos* 119(11):6376–6392
- Morris KI, Chan A, Ooi MC, Oozeer MY, Abakr YA, Morris KJK (2016) Effect of vegetation and waterbody on the garden city concept: an evaluation study using a newly developed city, Putrajaya, Malaysia. *Comput Environ Urban Syst* 58:39–51
- Nemunaitis-Berry KL, Klein PM, Basara JB, Fedorovich E. (2017) Sensitivity of Predictions of the Urban Surface Energy Balance and Heat Island to Variations of Urban Canopy Parameters in Simulations with the WRF Model. *J Appl Meteor Climatol* 56(3): 573–595
- Ohashi Y, Genchi Y, Kondo H, Kikegawa Y, Yoshikado H, Hirano Y (2007) Influence of air-conditioning waste heat on air temperature in Tokyo during summer: numerical experiments using an urban canopy model coupled with a building energy model. *J Appl Meteor Climatol* 46(1):66–81
- Oke TR (1981) Canyon geometry and the nocturnal urban heat island: comparison of scale model and field observations. *J Climatol* 1(3): 237–254
- Oke, T. R. (1987). *Boundary layer climates* Routledge.
- Oleson KW, Lawrence DM, Gordon B, Flanner MG, Kluzek E, Peter J, et al. (2010) Technical description of version 4.0 of the community land model (CLM).
- Pesaresi, M., Ehrlich, D., Ferri, S., Florczyk, A., Freire, S., Halkia, M., et al. (2016). Operating procedure for the production of the global human settlement layer from landsat data of the epochs 1975, 1990, 2000, and 2014. Publications Office of the European Union, JRC Technical Reports, 1–62.
- Pigeon G, Zibouche K, Bueno B, Le Bras J, Masson V (2014) Improving the capabilities of the town energy balance model with up-to-date building energy simulation algorithms: an application to a set of representative buildings in Paris. *Energy Buildings* 76:1–14
- Redon EC, Lemonsu A, Masson V, Morille B, Musy M (2017) Implementation of street trees within the solar radiative exchange

- parameterization of TEB in SURFEX v8. 0. *Geosci Model Dev* 10(1):385–411
- Revi A, Satterthwaite D, Aragón-Durand F, Corfee-Morlot J, Kiunsi R, Pelling M et al (2014) Urban areas. In: Balbus J, Cardona O (eds) *Climate change 2014: Impacts, adaptation, and vulnerability. Part A: global and sectoral aspects. Contribution of working group II to the fifth assessment report of the intergovernmental panel on climate change*. Cambridge University Press, pp 535–612
- Roth M (2000) Review of atmospheric turbulence over cities. *Q J R Meteorol Soc* 126(564):941–990
- Sabo F, Corbane C, Florczyk AJ, Ferri S, Pesaresi M, Kemper T (2018) Comparison of built-up area maps produced within the global human settlement framework. *Trans GIS* 22(6):1406–1436
- Sailor DJ (2011) A review of methods for estimating anthropogenic heat and moisture emissions in the urban environment. *Int J Climatol* 31(2):189–199
- Salamanca F, Krpo A, Martilli A, Clappier A (2010) A new building energy model coupled with an urban canopy parameterization for urban climate simulations—part I. formulation, verification, and sensitivity analysis of the model. *Theoretical Appl Climatol* 99(3–4):331
- Salamanca F, Martilli A, Tewari M, Chen F (2011) A study of the urban boundary layer using different urban parameterizations and high-resolution urban canopy parameters with WRF. *J Appl Meteorol Climatol* 50(5):1107–1128
- Santamouris M (2014) Cooling the cities—a review of reflective and green roof mitigation technologies to fight heat island and improve comfort in urban environments. *Sol Energy* 103:682–703
- Santamouris M, Ban-Weiss G, Osmond P, Paolini R, Synnefa A, Cartalis C, Muscio A, Zinzi M, Morakinyo TE, Ng E, Tan Z, Takebayashi H, Sailor D, Crank P, Taha H, Pisello AL, Rossi F, Zhang J, Kolokotsa D (2018) Progress in urban greenery mitigation science—assessment methodologies advanced technologies and impact on cities. *J Civ Eng Manag* 24(8):638–671
- Schoetter R, Masson V, Bourgeois A, Pellegrino M, Lévy J (2017) Parametrisation of the variety of human behaviour related to building energy consumption in the town energy balance (SURFEX-TEB v. 8.2). *Geosci Model Dev* 10(7):2801–2831
- Shaffer SR, Chow WTL, Georgescu M, Hyde P, Jenerette GD, Mahalov A, Moustouli M, Ruddell BL (2015) Multiscale Modeling and Evaluation of Urban Surface Energy Balance in the Phoenix Metropolitan Area. *J Appl Meteorol Climatol* 54(2):322–338
- Shashua-Bar L, Hoffman ME (2000) Vegetation as a climatic component in the design of an urban street: an empirical model for predicting the cooling effect of urban green areas with trees. *Energy Buildings* 31(3):221–235
- Shelton B, Karakiewicz J, Kvan T (2011) *The making of Hong Kong: From vertical to volumetric*. Routledge, New York
- Stewart ID, Oke TR (2012) Local climate zones for urban temperature studies. *Bull Am Meteorol Soc* 93(12):1879–1900
- Tian Y, Zhou W, Qian Y, Zheng Z, Yan J (2019) The effect of urban 2D and 3D morphology on air temperature in residential neighborhoods. *Landsc Ecol* 34(5):1161–1178
- Tornay N, Schoetter R, Bonhomme M, Faraut S, Masson V (2017) GENIUS: a methodology to define a detailed description of buildings for urban climate and building energy consumption simulations. *Urban Clim* 20:75–93
- Tse JWP, Yeung PS, Fung JC, Ren C, Wang R, Wong MM et al (2018) Investigation of the meteorological effects of urbanization in recent decades: a case study of major cities in Pearl River Delta. *Urban Clim* 26:174–187
- Vahmani P, Ban-Weiss G (2016) Impact of remotely sensed albedo and vegetation fraction on simulation of urban climate in WRF-urban canopy model: a case study of the urban heat island in Los Angeles. *J Geophys Res Atmos* 121(4):1511–1531
- Wang X, Liao J, Zhang J, Shen C, Chen W, Xia B, Wang T (2014) A numeric study of regional climate change induced by urban expansion in the Pearl River Delta, China. *J Appl Meteorol Climatol* 53(2):346–362
- Wang Y, Di Sabatino S, Martilli A, Li Y, Wong M, Gutiérrez E et al (2017) Impact of land surface heterogeneity on urban heat island circulation and sea-land breeze circulation in Hong Kong. *J Geophys Res Atmos* 122(8):4332–4352
- Wang R, Ren C, Xu Y, Lau KK, Shi Y (2018a) Mapping the local climate zones of urban areas by GIS-based and WUDAPT methods: a case study of Hong Kong. *Urban Clim* 24:567–576
- Wang Y, Li Y, Di Sabatino S, Martilli A, Chan PW (2018b) Effects of anthropogenic heat due to air-conditioning systems on an extreme high temperature event in Hong Kong. *Environ Res Lett*
- Wong LT, Mui KW, Shi KL (2008) Energy impact of indoor environmental policy for air-conditioned offices of Hong Kong. *Energy Policy* 36(2):714–721
- Wong WS (2014) Architectural phenomena following law-review of residential buildings in Hong Kong. *J Civil Eng Architect Res* 1(4): 215–229
- Wong MS, Yang J, Nichol J, Weng Q, Menenti M, Chan PW (2015) Modeling of anthropogenic heat flux using HJ-1B Chinese small satellite image: a study of heterogeneous urbanized areas in Hong Kong. *IEEE Geosci Remote Sens Lett* 12(7):1466–1470
- Wong MM, Fung JC, Ching J, Yeung PPS, Tse JWP, Wang R et al (2019) Evaluation of uWRF performance and modeling guidance based on WUDAPT and NUDAPT UCP datasets for Hong Kong. *Urban Climate News* 71:17–21
- Zhao, D., & Wu, J. (2018). Changes in urban-related precipitation in the summer over three city clusters in China. *Theoretical Appl Climatol*, 1–11

Publisher's note Springer Nature remains neutral with regard to jurisdictional claims in published maps and institutional affiliations.